

Tripodal Aminophenolate Ligand Complexes of Aluminum(III), Gallium(III), and Indium(III) in Water

P. Caravan and Chris Orvig*

Department of Chemistry, University of British Columbia, 2036 Main Mall,
Vancouver, British Columbia, Canada V6T 1Z1

Received October 10, 1996[Ⓞ]

Four water-soluble amine phenols have been prepared: tris(((2-hydroxy-5-sulfobenzyl)amino)ethyl)amine (H₆-TRNS), 1,1,1-tris(((2-hydroxy-5-sulfobenzyl)amino)methyl)ethane (H₆TAMS), 1,2,3-tris((2-hydroxy-5-sulfobenzyl)-amino)propane (H₆TAPS), and *cis,cis*-1,3,5-tris((2-hydroxy-5-sulfobenzyl)amino)cyclohexane (H₆TACS). Complex formation constants have been measured at 25 °C ($\mu = 0.16$ M NaCl): $\log K [M(\text{TRNS})]^{3-} ([M(\text{HTRNS})]^{2-}) M = \text{Ga } 28.55 (36.90), \text{In } 29.3 (34.9); \log K [M(\text{TAMS})]^{3-} ([M(\text{HTAMS})]^{2-}) M = \text{Al } 22.5 (29.3), \text{Ga } 31.83, \text{In } 28.49; \log K [M(\text{TAPS})]^{3-} ([M(\text{HTAPS})]^{2-}) M = \text{Al } 22.8 (29.0), \text{Ga } 31.54 (35.15), \text{In } 27.56 (31.93)$. The order of stability is Ga(III) > In(III) > Al(III) for H₆TAMS and H₆TAPS, while for H₆TRNS it is Ga(III) \approx In(III) > Al(III). The solution structures of the complexes have been probed by multinuclear NMR (¹H, ¹³C, ²⁷Al, ⁷¹Ga, ¹¹⁵In) and UV spectroscopic studies, and these solution structures are compared with solid state structures for analogous complexes. The ¹H NMR spectrum in D₂O establishes TAPS to be preorganized for metal ion binding. H₆TACS exists in the wrong conformation for metal ion binding, and this results in slow complexation kinetics and relatively weaker binding.

Introduction

In the quest for new chelators of gallium and indium with the intent of developing radiopharmaceuticals based on ⁶⁷Ga, ⁶⁸Ga, or ¹¹¹In, it is germane to employ a multidentate ligand. A hexadentate ligand offers two advantages: a higher thermodynamic stability than its bi- or tridentate analogues and a metal complex stability indifferent to a dilution effect, important considering the low concentrations (nM) involved in nuclear medicine. The gallium or indium complex should be stable with respect to both hydrolysis and demetalation by the serum protein transferrin. As the radionuclides involved are short lived, rapid complexation kinetics when labeling are desirable, while demetalation kinetics should be slow. Another useful characteristic is the ease of modification of the ligand backbone in order to change the lipophilicity of the complex (and possibly its biodistribution) or to tag the complex to a biologically important molecule (antibody, protein, etc.) via a bifunctional linkage.

Harris and co-workers have determined binding constants for a variety of metal ions with the human serum protein transferrin.^{1–3} For tripositive metal ions, such as gallium and indium, transferrin is the dominant endogenous chelating agent in the blood. A comparison of binding constants between the metal chelate proposed for radiopharmaceutical trial and the transferrin metal complex would offer a rational approach to radiopharmaceutical screening, and this approach has been employed successfully by Martell, Welch, and co-workers.^{4,5}

The same principles apply to Al(III) sequestration. Aluminum, a nonessential element, can cause neurotoxicity and dialysis encephalopathy and has been shown to accumulate in

some of the hallmark lesions of Alzheimer's Disease.⁶ The only approved chelator for aluminum(III) overload is the tris-(hydroxamate) siderophore desferrioxamine, an O₆ donor. It has been recognized that the most effective ligands for Al(III) chelation are O-donor ligands⁷ and that the stability of Al(III) complexes generally decreases via the replacement of O-donor groups with N-donor groups.⁸ Consequently, the aqueous coordination chemistry of Al(III) with O,N-donor ligands is not nearly so well established as is that of Ga(III) and In(III), both of which have higher affinities for the neutral nitrogen donor.⁹ The aminophenolates reported in this study, while unlikely to present themselves as efficient Al(III) chelators for clinical application, will serve to further the understanding of aqueous Al(III) coordination chemistry by addressing a number of factors.

There are a variety of topologies available for the design of a multidentate ligand: macrocycles, macrobicycles, macrocycles with pendant donors, and linear, branched, and tripod ligands¹⁰ (Scheme 1). Because of its cyclic nature, a macrocycle-derived ligand generally offers more selectivity for a metal ion of the appropriate ionic radius. Macrocycle-based ligands also offer high-thermodynamic stability (macrocycle effect);¹¹ while the metalation kinetics are often slower than that for a nonmacro-cyclic analog, the demetalation kinetics are even slower.¹² In contrast, flexible linear and branched ligands often bind rapidly, but a consequence of their flexibility is indiscriminate metal binding and more rapid demetalation. With the tripodal ligand,

(6) Doll, R. *Age Ageing* **1993**, 22, 138.

(7) Martell, A. E.; Motekaitis, R. J.; Smith, R. M. *Polyhedron* **1990**, 9, 171.

(8) Clevette, D. J.; Orvig, C. *Polyhedron* **1990**, 9, 151.

(9) Martell, A. E.; Smith, R. M. *Critical Stability Constants*; Plenum: New York, 1974–1989; Vol. 1–6.

(10) Martell, A. E.; Hancock, R. D. *Metal Complexes in Aqueous Solution*; Plenum: New York, 1996.

(11) Cabiness, D. K.; Margerum, D. W. *J. Am. Chem. Soc.* **1969**, 91, 6540.

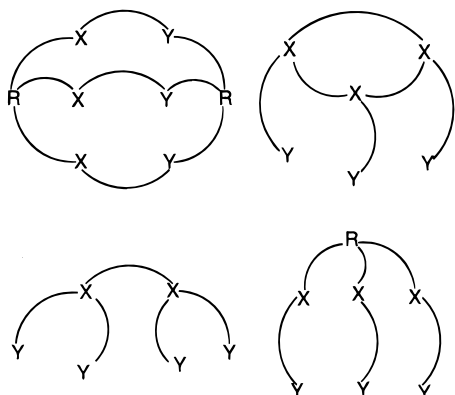
(12) Lindoy, L. F. *The Chemistry of Macrocyclic Ligand Complexes*; Cambridge University Press: Cambridge, 1989.

* To whom correspondence should be addressed. Tel: 604-822-4449. Fax: 604-822-2847. E-mail: orvig@chem.ubc.ca.

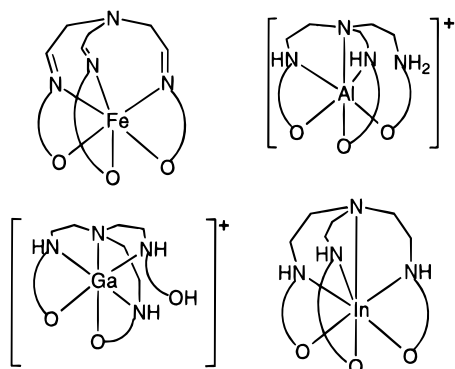
[Ⓞ] Abstract published in *Advance ACS Abstracts*, December 15, 1996.

- (1) Harris, W. R.; Pecoraro, V. L. *Biochemistry* **1983**, 22, 292.
- (2) Harris, W. R.; Sheldon, J. *Inorg. Chem.* **1990**, 29, 119.
- (3) Harris, W. R.; Chen, Y. C.; Wein, K. *Inorg. Chem.* **1994**, 33, 4991.
- (4) Mathias, C. J.; Sun, Y.; Welch, M. J.; Green, M. A.; Thomas, J. A.; Wade, K. R.; Martell, A. E. *Nucl. Med. Biol.* **1988**, 15, 69.
- (5) Motekaitis, R. J.; Martell, A. E.; Welch, M. J. *Inorg. Chem.* **1990**, 29, 1463.

Scheme 1



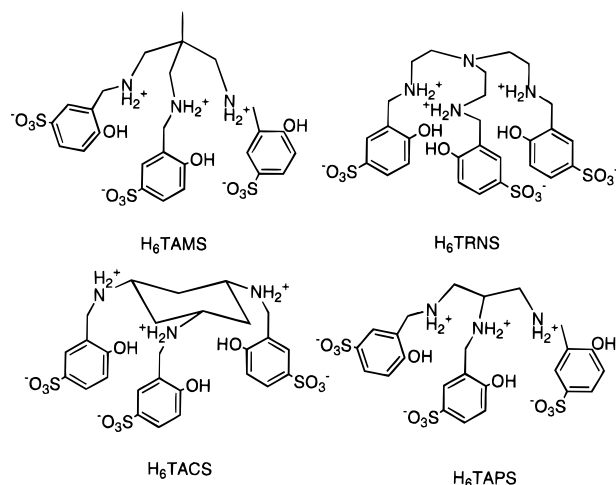
Scheme 2



a combination of the favorable properties of both acyclic and cyclic ligands may be realized.

This approach has been taken with Schiff bases derived from various tripodal amines.^{13–15} There is the wide array of substituted salicylaldehydes available to potentially alter the biodistribution. Furthermore, the Schiff base condensation reaction is rapid, is clean, and gives high yields. Although metalated Schiff base complexes generally have a low aqueous solubility, Evans and Jakubovic have studied complexes derived from the condensation of sodium 5-sulfosalicylaldehyde with various amines and determined *pM* values as a measure of thermodynamic stability.^{16,17} One drawback to Schiff bases is that they undergo partial hydrolysis in water at the imine linkage, and this may be the source of *in vivo* degradation of their metal complexes. Reduction of the imine eliminates the hydrolysis problem and results in a more flexible ligand. In the case of the Schiff base saltren (the Fe complex of which is depicted schematically in Scheme 2), the reduced form of the ligand resulted in three different coordination geometries with Al(III), Ga(III), and In(III);¹⁸ each geometry differed from the analogous saltren complexes.¹⁹ This diversity was a consequence of employing a ligand with seven potential donors. Ligands with potential N₃O₃ donor sets (e.g., nonsulfonated analogs of H₆TAMS and H₆TAPS in Scheme 3) give the expected octahedral group 13 metal complexes.^{20,21} Previous work in this laboratory

Scheme 3



has involved the synthesis and characterization of amine phenols derived from the amines tren (tris(aminoethyl)amine),¹⁸ tame (tris(aminomethyl)ethane),²¹ and tap (triaminopropane)²⁰ and their aluminum, gallium, and indium complexes.^{18,20,21} Roundhill and co-workers have adopted the same approach using the amine *cis,cis*-1,3,5-triaminocyclohexane and ubiquitously reported the Al(III), Ga(III), In(III), and Fe(III) complexes.^{22–24}

This work explores the effect of backbone variations on the selectivity of multidentate aminophenolate ligands among the trivalent metal ions Al(III), Ga(III), and In(III) in water. The study involves the preparation of the 5-sulfonic acid derivatives of the amine phenols (to ensure aqueous solubility) shown in Scheme 3, the *in situ* characterization of the Al(III), Ga(III), and In(III) complexes, the determination of ligand deprotonation constants, and the determination of metal complex formation constants.

Experimental Section

Materials. Sodium borohydride, tris(2-aminoethyl)amine (tren), salicylaldehyde, aniline, tris(hydroxymethyl)ethane, sodium azide, lithium aluminum hydride, diethylene glycol, glycerin, *cis,cis*-1,3,5-cyclohexanetriol, sodium deuterioxide (NaOD, 40%), deuterium chloride (DCl, 12 M), and the aluminum, gallium, and indium atomic absorption standards were obtained from Aldrich. Hydrated aluminum, gallium, and indium nitrates were obtained from Alfa. Deuterium oxide (D₂O) was purchased from Isotec. Anhydrous sodium carbonate was obtained from BDH. All were used without further purification. Sodium 5-sulfosalicylaldehyde,²⁵ tris(aminomethyl)ethane (tame),²¹ triaminopropane (tap),²⁶ and *cis,cis*-1,3,5-triaminocyclohexane (tach)²⁷ were prepared according to literature preparations.

Instrumentation. ¹H NMR (200 and 300 MHz) and ¹³C NMR (50.3 and 75.5 MHz) spectra were referenced to TMS and recorded on Bruker AC-200E and Varian XL 300 spectrometers, respectively. ²⁷Al, ⁷¹Ga, and ¹¹⁵In NMR spectra were recorded on the Varian XL 300

(13) Green, M. A.; Welch, M. J.; Huffman, J. C. *J. Am. Chem. Soc.* **1984**, *106*, 3689.

(14) Green, M. A.; Welch, M. J.; Mathias, C. J.; Fox, K. A. A.; Knabb, R. M.; Huffman, J. C. *J. Nucl. Med.* **1985**, *26*, 170.

(15) Green, M. A. *J. Labelled Comp. Radiopharm.* **1986**, *23*, 1227.

(16) Evans, D. F.; Jakubovic, D. A. *Polyhedron* **1988**, *7*, 1881.

(17) Evans, D. F.; Jakubovic, S. A. *J. Chem. Soc., Dalton Trans.* **1988**, 2927.

(18) Liu, S.; Rettig, S. J.; Orvig, C. *Inorg. Chem.* **1992**, *31*, 5400.

(19) Cook, D. F.; Cummins, D.; McKenzie, E. D. *J. Chem. Soc., Dalton Trans.* **1976**, 1369.

(20) Liu, S.; Wong, E.; Rettig, S. J.; Orvig, C. *Inorg. Chem.* **1993**, *32*, 4268.

(21) Liu, S.; Wong, E.; Karunaratne, V.; Rettig, S. J.; Orvig, C. *Inorg. Chem.* **1993**, *32*, 1756.

(22) Bollinger, J. E.; Mague, J. T.; Roundhill, D. M. *Inorg. Chem.* **1994**, *33*, 1241.

(23) Bollinger, J. E.; Mague, J. T.; O'Connor, C. J.; Banks, W. A.; Roundhill, D. M. *J. Chem. Soc., Dalton Trans.* **1995**, 1677.

(24) Bollinger, J. E.; Mague, J. T.; Banks, W. A.; Kastin, A. J.; Roundhill, D. M. *Inorg. Chem.* **1995**, *34*, 2143.

(25) Botsivali, M.; Evans, D. F.; Missen, P. H.; Upton, M. W. *J. Chem. Soc., Dalton Trans.* **1985**, 1147.

(26) Henrick, K.; McPartlin, M.; Munjoma, S.; Owston, P. G.; Peters, R.; Sangokoya, S. A.; Tasker, P. A. *J. Chem. Soc., Dalton Trans.* **1982**, 225.

(27) Fleisher, E. B.; Gebala, A. E.; Levey, A.; Tasker, P. A. *J. Org. Chem.* **1971**, *36*, 3042.

spectrometer at 78.2, 91.5, and 65.7 MHz, respectively, and were referenced to the appropriate 0.1 M metal nitrate in 6 M nitric acid. Mass spectra were obtained with a Kratos Concept II H32Q (Cs⁺, LSIMS) instrument. UV-vis spectra were recorded on a Shimadzu UV-2100. Infrared spectra were obtained as KBr disks in the range 4000–400 cm⁻¹ on a Galaxy Series FTIR 5000 spectrophotometer and were referenced to polystyrene. Analyses of C, H, and N were performed by Mr. Peter Borda in this department. Melting points were measured on a Mel-Temp apparatus and are uncorrected.

Trisodium Tris(((2-hydroxy-5-sulfonatobenzylidene)amino)ethyl)amine (Na₃saltrens). To a suspension of sodium sulfosalicylaldehyde (6.72 g, 30 mmol) in methanol (150 mL) was added tren (1.46 g, 10 mmol). This suspension immediately turned from a pale yellow to a brilliant canary yellow. The mixture was allowed to stir for an hour, after which time it was cooled to 4 °C in the refrigerator. The fine bright yellow powder was collected on a Büchner funnel and washed with ethanol (10 mL), followed by ether (10 mL). Yield: 5.61 g (83%). ¹H NMR (300 MHz, DMSO-*d*₆): 2.88 (s, 6H, ethylenic CH₂), 3.66 (s, 6H, ethylenic CH₂), 6.78 (d, 3H, ring H(3), ³J = 9.3 Hz), 7.55 (dd, 3H, ring H(4), ³J = 9.3 Hz, ⁴J = 2.3 Hz), 7.69 (d, 3H, ring H(6), ⁴J = 2.3 Hz), 8.53 (s, 3H, imine CH) ppm. ¹³C NMR (50.3 MHz, DMSO-*d*₆): 54.87, 56.32, 116.41, 116.99, 129.15, 130.22, 138.17, 162.42, 165.55 ppm. Mass spectrum (LSIMS): *m/z* 743 ([M - Na + 2H]⁺, [C₂₇H₂₉N₄Na₂O₁₂S₃]⁺), 765 ([M + H]⁺, [C₂₇H₂₈N₄Na₃O₁₂S₃]⁺), 787 ([M + Na]⁺, [C₂₇H₂₇N₄Na₄O₁₂S₃]⁺). IR (cm⁻¹, KBr disk): 3600–3400 (b s, ν_{O-H}), 1642 (s, ν_{C=N}), 1518 (s, ν_{C=C}), 1186 (vs, ν_{S=O}), 1107, 1035 (s, ν_{C-C}).

Tris(((2-hydroxy-5-sulfobenzyl)amino)ethyl)amine Monohydrate (H₆TRNS·H₂O). Sodium borohydride (1.6 g, 4 mmol) was added to a suspension of saltrens (7.65 g, 1.0 mmol) in methanol over a period of 30 min. After the addition was complete, the solvent was removed to give a white solid. Methanol (60 mL) was added and removed under reduced pressure. This was repeated twice more. The resultant solid was dissolved in a minimal amount of water (15 mL), and the pH was adjusted to about 2 with concentrated HCl; a white solid precipitated and was collected on a Büchner funnel. It was purified by redissolving it in a mildly basic solution (pH ~ 8), filtering, and acidifying the filtrate to give a white precipitate as the zwitterion. This was filtered and dried overnight *in vacuo* at 95 °C to yield 5.0 g (71%); mp > 250 °C. Anal. Calcd (Found) for C₂₇H₃₆N₄O₁₂S₃·H₂O: C, 44.87 (44.86); H, 5.30 (5.46); N, 7.75 (7.59). Potentiometric analysis was consistent with this formulation. ¹H NMR (200 MHz, D₂O, pD = 7.1): 2.80 (t, 6H, ethylenic CH₂, ³J = 6 Hz), 3.08 (t, 6H, ethylenic CH₂, ³J = 6 Hz), 4.18 (s, 6H, benzylic CH₂), 6.70 (d, 3H, ring H(3), ³J = 9 Hz), 7.61 (dd, 3H, ring H(4), ³J = 9 Hz, ⁴J = 1 Hz), 7.63 (d, 3H, ring H(6), ⁴J = 1 Hz) ppm. ¹³C NMR (75.48 MHz, D₂O, pD = 8.0): 45.99, 51.81, 52.06, 121.54, 122.47, 130.67, 130.81, 130.89, 170.42 ppm. Mass spectrum (LSIMS): *m/z* 705 ([M + H]⁺, [C₂₇H₃₆N₄O₁₂S₃]⁺). IR (cm⁻¹, KBr disk): 3500–2600 (b s, ν_{N-H}, ν_{O-H}), 1730 (m, δ_{N-H}), 1604 (s, δ_{N-H}), 1502, 1442, 1375 (s, ν_{C=C}), 1200 (vs, ν_{S=O}). UV (λ_{max}, nm (ε, M⁻¹ cm⁻¹)): pH = 2 276 (4800), 232 (26 000), 203 (72 000); pH = 12 290 (11 000), 256 (47 000). It is slightly soluble in acid and soluble in neutral to basic pH.

Trisodium 1,1,1-Tris(((2-hydroxy-5-sulfonatobenzylidene)amino)methyl)ethane (Na₃saltams). To a suspension of sodium 5-sulfosalicylaldehyde (6.72 g, 30 mmol) in methanol (150 mL) at room temperature was added tame (1.10 g, 10 mmol) in 10 mL of methanol. The pale yellow suspension immediately brightened to a lemon yellow hue. The suspension was stirred for an hour, and then the suspension was cooled to 4 °C in the refrigerator while a lemon colored powder deposited. The powder was collected on a Büchner funnel, washed with ethanol (10 mL), washed with ether (10 mL), and dried overnight *in vacuo*. Yield: 6.00 g (82%). ¹H NMR (300 MHz, DMSO-*d*₆): 1.04 (s, 3H, methyl CH₃), 3.62 (s, 6H, methylenic CH₂), 6.86 (d, 3H, ring H(3), ³J = 9.3 Hz), 7.58 (dd, 3H, ring H(4), ³J = 9.3 Hz, ⁴J = 2.3 Hz), 7.73 (d, 3H, ring H(6), ⁴J = 2.3 Hz), 8.66 (s, 3H, imine CH) ppm. ¹³C NMR (75.48 MHz, DMSO-*d*₆): 20.03, 63.78, 115.76, 117.23, 129.03, 130.03, 139.08, 160.96, 167.25 ppm. Mass spectrum (LSIMS): *m/z* 670 ([M - 3Na + 4H]⁺, [C₂₆H₂₈N₃O₁₂S₃]⁺), 692 ([M - 2Na + 3H]⁺, [C₂₆H₂₇N₃NaO₁₂S₃]⁺), 714 ([M - Na + 2H]⁺, [C₂₆H₂₆N₃Na₂O₁₂S₃]⁺), 736 ([M + H]⁺, [C₂₆H₂₅N₃Na₃O₁₂S₃]⁺), 758 ([M

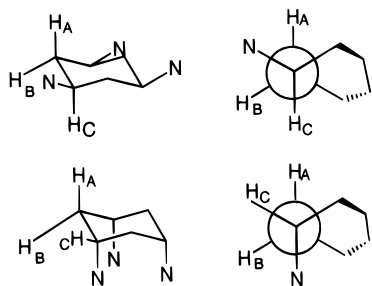
+ Na]⁺, [C₂₆H₂₄N₃Na₄O₁₂S₃]⁺). IR (cm⁻¹, KBr disk): 3450 (b s, ν_{O-H}), 1639 (s, ν_{C=N}), 1484 (m, ν_{C=C}), 1191 (vs, ν_{S=O}), 1111, 1039 (s, ν_{C-C}).

1,1,1-Tris(((2-hydroxy-5-sulfobenzyl)amino)methyl)ethane Dihemihydrate (H₆TAMS·2.5H₂O). Methanol (60 mL) was cooled to 0 °C in an ice bath, and sodium borohydride (0.11 g, 2.9 mmol) was added with stirring. To this was added Na₃saltams (0.54 g, 0.74 mmol) in small portions (~50 mg each). After each portion was added, the reaction was allowed to proceed until all of the solid Schiff base had dissolved and the bright yellow color dissipated. After all of the Na₃saltams had been added (~1 h), the solution was allowed to stir for an hour. The solution was then acidified with 6 M HCl, which gave a white precipitate. The methanol was then boiled down to 20 mL, another 100 mL of methanol was added, and the methanol was again boiled down to 20 mL. The white suspension was allowed to cool to room temperature, and the white solid was collected on a medium frit. The white solid was then dissolved in water, and this solution was passed down a Rexyn 101 cation exchange column (H⁺ form) and eluted with deionized distilled water until the eluant was no longer acidic. Solvent was removed from the eluant under reduced pressure at 65 °C to give a white solid. The solid was dried at 95 °C *in vacuo* overnight to yield 0.35 g (71%); mp > 250 °C. Anal. Calcd (Found) for C₂₆H₃₃N₃O₁₂S₃·2.5H₂O: C, 43.33 (43.23); H, 5.31 (5.21); N, 7.83 (7.68). Potentiometric analysis was consistent with this formulation. ¹H NMR (200 MHz, D₂O, pD = 12): 2.80 (t, 6H, ethylenic CH₂, ³J = 6 Hz), 3.08 (t, 6H, ethylenic CH₂, ³J = 6 Hz), 4.18 (s, 6H, benzylic CH₂), 6.70 (d, 3H, ring H(3), ³J = 9 Hz), 7.61 (dd, 3H, ring H(4), ³J = 9 Hz, ⁴J = 1 Hz), 7.63 (d, 3H, ring H(6), ⁴J = 1 Hz) ppm. ¹³C NMR (75.48 MHz, D₂O, pD = 12): 22.55, 40.02, 52.78, 57.04, 121.13, 128.75, 129.01, 129.63, 130.38, 171.73 ppm. Mass spectrum (LSIMS): *m/z* 676 ([M + H]⁺, [C₂₆H₃₄N₃O₁₂S₃]⁺). IR (cm⁻¹, KBr disk): 3500–2600 (b s, ν_{N-H}, ν_{O-H}), 1604 (s, δ_{N-H}), 1501, 1433 (s, ν_{C=C}), 1210 (vs, ν_{S=O}), 1100, 1033 (s, ν_{C-C}). UV (λ_{max}, nm (ε, M⁻¹ cm⁻¹)): pH = 2 276 (4420), 232 (31 000); pH = 12 288 (10 400), 256 (52 000). It is soluble in water and hot DMSO.

Trisodium 1,2,3-Tris(2-hydroxy-5-sulfonatobenzylidene)amino)propane (Na₃saltaps). To a suspension of sodium 5-sulfosalicylaldehyde (6.72 g, 30 mmol) in methanol (150 mL) at room temperature was added tap (0.90 g, 10 mmol) in 10 mL of methanol. The pale yellow suspension immediately became bright yellow. The suspension was stirred for an hour, and then the suspension was cooled to 4 °C in the refrigerator while a bright yellow colored powder deposited. The powder was collected on a Büchner funnel, washed with ethanol (10 mL), washed with ether (10 mL), and dried overnight *in vacuo*. Yield: 5.80 g (82%). ¹H NMR (200 MHz, DMSO-*d*₆): 3.38 (m, 1H, methine CH), 3.98 (s, 4H, methylenic CH₂), 6.82 (d, 2H, ring H(3), ³J = 9.67 Hz), 6.83 (d, 1H, ring H(3'), ³J = 9.33 Hz), 7.55 (dd, 2H, ring H(4), ³J = 9.67 Hz, ⁴J = 2.0 Hz), 7.56 (dd, 1H, ring H(4'), ³J = 9.33 Hz, ⁴J = 2.0 Hz), 7.71 (d, 3H, ring H(6) and ring H(6'), ⁴J = 2.0 Hz), 8.68 (s, 2H, imine CH), 8.70 (s, 1H, imine CH center arm) ppm. ¹³C NMR (75.5 MHz, DMSO-*d*₆): 60.94, 68.57, 115.77, 117.03, 117.09, 128.90, 128.94, 129.97, 130.04, 138.86, 138.94, 160.65, 160.86, 166.63, 167.38 ppm. Mass spectrum (LSIMS): *m/z* 664 ([M - 2Na + 3H]⁺, [C₂₄H₂₃N₃NaO₁₂S₃]⁺), 686 ([M - Na + 2H]⁺, [C₂₄H₂₂N₃Na₂O₁₂S₃]⁺), 708 ([M + H]⁺, [C₂₆H₂₁N₃Na₃O₁₂S₃]⁺), 730 ([M + Na]⁺, [C₂₆H₂₀N₃Na₄O₁₂S₃]⁺). IR (cm⁻¹, KBr disk): 3456 (b s, ν_{O-H}), 1638 (s, ν_{C=N}), 1514, 1492 (m, ν_{C=C}), 1190 (vs, ν_{S=O}), 1108, 1036 (s, ν_{C-C}).

1,2,3-Tris(2-hydroxy-5-sulfobenzyl)amino)propane Dihemihydrate (H₆TAPS·2.5H₂O). Methanol (100 mL) was cooled to 0 °C in an ice bath, and sodium borohydride (0.45 g, 12.0 mmol) was added with stirring. To this was added Na₃saltaps (2.1 g, 3.0 mmol) in small portions (~10 mg). After each portion was added, the reaction was allowed to proceed until all of the solid Schiff base had dissolved and the bright yellow color dissipated. After all of the Na₃saltaps had been added (~1 h), the solution was allowed to stir for an hour. The solution was then acidified with 6 M HCl; this gave a white precipitate. The methanol was then boiled down to 20 mL, another 100 mL of methanol was added, and the methanol was again boiled down to 20 mL. The white suspension was allowed to cool to room temperature, and the white solid was collected on a medium frit. The white solid was then dissolved in water, and this solution was passed down a Rexyn 101 cation exchange column (H⁺ form) and eluted with deionized distilled water until the eluant was no longer acidic. The solvent was removed

Scheme 4



from the eluant under reduced pressure at 65 °C to give a white solid. The solid was dried at 95 °C *in vacuo* overnight to yield 1.00 g (49%); mp > 250 °C. Anal. Calcd (Found) for C₂₄H₃₉N₃O₁₂S₃·2.5H₂O: C, 41.61 (41.72); H, 4.95 (4.70); N, 6.07 (6.05). Potentiometric analysis was consistent with this formulation. ¹H NMR (200 MHz, D₂O, pD = 12): 2.60 (d, 4H, methylenic CH₂, ³J = 5.7 Hz), 2.91 (q, 1H, methine CH, ³J = 5.7 Hz), 3.63 (s, 6H, benzylic CH₂), 6.58 (d, 3H, ring H(3), ³J = 9.3 Hz), 7.42 (dd, 3H, ring H(4), ³J = 9.3 Hz, ⁴J = 2.7 Hz), 7.47 (d, 3H, ring H(6), ⁴J = 2.7 Hz) ppm. ¹³C NMR (75.48 MHz, D₂O, pD = 12): 49.70, 51.99, 52.95, 59.05, 121.17, 121.30, 128.79, 128.87, 129.07, 129.20, 129.61, 129.94, 130.46, 130.51, 171.57, 171.70 ppm. Mass spectrum (LSIMS): *m/z* 648 ([M + H]⁺, [C₂₆H₃₄N₃O₁₂S₃]⁺). IR (cm⁻¹, KBr disk): 3500–2600 (b s, ν_{N-H}, ν_{O-H}), 1611 (s, δ_{N-H}), 1493, 1439 (s, ν_{C=C}), 1210, 1170 (vs, ν_{S=O}), 1100, 1033 (s, ν_{C-C}). UV (λ_{max}, nm (ε, M⁻¹ cm⁻¹): pH = 2 277 (4400), 232 (28 900); pH = 12 288 (11 800), 256 (47 000). It is soluble in water and hot DMSO.

Trisodium *cis,cis*-1,3,5-Tris(2-hydroxy-5-sulfonatobenzylidene)-aminocyclohexane (Na₃saltachs). To a suspension of sodium 5-sulfosalicylaldehyde (2.13 g, 9.5 mmol) in methanol (50 mL) at room temperature was added tach (0.41 g, 10 mmol) in 10 mL of methanol. The pale yellow suspension immediately brightened to a lemon yellow hue and was dissolved with stirring. The solution was stirred for an hour, 50 mL of absolute ethanol was added, and the suspension was cooled to 4 °C in the refrigerator while a lemon colored powder deposited. The powder was collected on a Büchner funnel, washed with ethanol (10 mL), washed with ether (10 mL), and dried overnight *in vacuo*. Yield: 1.90 g (80%). ¹H NMR (200 MHz, DMSO-*d*₆, see Scheme 4): 1.81 (q, 3H, H(A_{ax}), ²J_{AB} = 12 Hz, ³J_{AC} = 12 Hz), 2.06 (d, 3H, H(B_{eq}), ²J_{AB} = 12 Hz, ³J_{BC} = 2.5 Hz), 3.72 (t, 3H, H(C_{eq}), ³J_{AC} = 12 Hz, ³J_{BC} = 2.5 Hz), 6.83 (d, 3H, ring H(3), ³J = 9.0 Hz), 7.57 (d, 3H, ring H(4), ³J = 9.0 Hz), 7.74 (s, 3H, ring H(6)), 8.72 (s, 3H, imine CH) ppm. ¹³C NMR (75.48 MHz, DMSO-*d*₆): 62.46, 115.68, 117.18, 128.96, 129.86, 138.89, 160.88, 164.60 ppm. Mass spectrum (LSIMS): *m/z* 682 ([M - 3Na + 4H]⁺, [C₂₇H₂₈N₃O₁₂S₃]⁺), 704 ([M - 2Na + 3H]⁺, [C₂₇H₂₇N₃NaO₁₂S₃]⁺), 726 ([M - Na + 2H]⁺, [C₂₇H₂₆N₃Na₂O₁₂S₃]⁺), 748 ([M + H]⁺, [C₂₇H₂₅N₃Na₃O₁₂S₃]⁺), 770 (M + Na)⁺, [C₂₇H₂₄N₃Na₄O₁₂S₃]⁺. IR (cm⁻¹, KBr disk): 3454 (b s, ν_{O-H}), 1639 (s, ν_{C=N}), 1524, 1382 (m, ν_{C=C}), 1186 (vs, ν_{S=O}), 1108, 1035 (s, ν_{C-C}).

***cis,cis*-1,3,5-Tris(2-hydroxy-5-sulfobenzylamino)cyclohexane Tetrahydrate (H₆TACS·4H₂O).** Methanol (100 mL) was cooled to 0 °C in an ice bath, and sodium borohydride (0.28 g, 7.4 mmol) was added with stirring. To this was added Na₃saltachs (1.30 g, 1.7 mmol) in small portions (~10 mg each). After each portion was added, the reaction was allowed to proceed until all of the solid Schiff base had dissolved and the bright yellow color dissipated. After all of the Na₃saltachs had been added (~1 h), the solution was heated to reflux and stirred for 30 min. The solution was then acidified with 6 M HCl, resulting in a white precipitate. The methanol was then boiled down to 20 mL, another 100 mL methanol was added, and the methanol was again boiled down to 20 mL. The white suspension was allowed to cool to room temperature, and the white solid was collected on a medium frit. The white solid was then dissolved in water, and this solution was passed down a Rexyn 101 cation exchange column (H⁺ form) and eluted with deionized distilled water until the eluant was no longer acidic. The solvent was removed from the eluant under reduced pressure at 65 °C to give a white solid. The solid was dried at 95 °C *in vacuo* overnight to yield 0.73 g (55%); mp > 250 °C. Anal. Calcd (Found) for C₂₄H₃₉N₃O₁₂S₃·4H₂O: C, 42.68 (42.89); H, 5.44 (5.40);

N, 5.53 (5.49). Potentiometric analysis was consistent with this formulation. ¹H NMR (200 MHz, D₂O, pD = 12, see Scheme 4): 0.97 (q, 3H, H(A_{ax}), ²J_{AB} = 11 Hz, ³J_{AC} = 11.7 Hz), 2.26 (d, 3H, H(B_{eq}), ²J_{AB} = 11 Hz, ³J_{BC} = 2.0 Hz), 2.67 (t, 3H, H(C_{eq}), ³J_{AC} = 11.7 Hz, ³J_{BC} = 2.0 Hz), 3.67 (s, 6H, benzylic CH₂), 6.56 (d, 3H, ring H(3), ³J = 8.6 Hz), 7.39 (dd, 3H, ring H(4), ³J = 8.6 Hz, ⁴J = 2.6 Hz), 7.46 (d, 3H, ring H(6), ⁴J = 2.6 Hz) ppm. ¹³C NMR (75.5 MHz, D₂O, pD = 12): 40.28, 43.71, 49.03, 55.37, 121.14, 128.72, 128.99, 129.54, 130.72, 171.53 ppm. Mass spectrum (LSIMS): *m/z* 688 ([M + H]⁺, [C₂₆H₃₄N₃O₁₂S₃]⁺). IR (cm⁻¹, KBr disk): 3500–2600 (b s, ν_{N-H}, ν_{O-H}), 1607 (s, δ_{N-H}), 1503, 1433 (s, ν_{C=C}), 1210, 1171 (vs, ν_{S=O}), 1101, 1033 (s, ν_{C-C}). UV (λ_{max}, nm (ε, M⁻¹ cm⁻¹): pH = 2 276 (4960), 232 (33 600); pH = 12 287 (12 000), 256 (48 800). It is soluble in water and hot DMSO.

Metal Complexes. The metal complexes of these sulfonated ligands were prepared *in situ*; no attempts were made to isolate them. However, many structural reports exist for the analogous nonsulfonated ligand metal complexes.^{18,20–24} The method used was the same in all instances, and the complexes were characterized by ¹H and in some cases ¹³C, ²⁷Al, ⁷¹Ga, or ¹¹⁵In NMR. As complex formation is pD dependent, the usual protocol for complex synthesis was to take the appropriate stoichiometry of metal nitrate and ligand precursor (30–50 mM) and adjust the pD to the desired level using NaOD or DCl solutions. In order to compare the spectral behavior (in D₂O) with the thermodynamic constants determined (in H₂O), the relationship pD = pH + 0.40 was used.²⁸

Na₃[Al(TAMS)]. ¹H NMR (300 MHz, D₂O, pD = 10.0): 0.68 (s, 3H, methyl CH₃), 2.58 (d, 3H, methylenic CH, ²J_{AB} = 14.3 Hz), 2.63 (d, 3H, methylenic CH, ²J_{AB} = 14.3 Hz), 3.27 (d, 3H, benzylic CH, ²J_{AB} = 13.5 Hz), 4.19 (d, 3H, benzylic CH, ²J_{AB} = 13.5 Hz), 6.86 (d, 3H, ring H(3), ³J = 8.4 Hz), 7.56 (d, 3H, ring H(6), ⁴J = 2.4 Hz), 7.67 (dd, 3H, ring H(4), ³J = 8.4 Hz, ⁴J = 2.4 Hz) ppm. ²⁷Al NMR (D₂O, pD = 10): δ = +5 ppm, W_{1/2} = 870 Hz.

Na₃[Ga(TAMS)]. ¹H NMR (300 MHz, D₂O, pD = 9.3): 0.69 (s, 3H, methyl CH₃), 2.69 (d, 3H, methylenic CH, ²J_{AB} = 13.3 Hz), 2.77 (d, 3H, methylenic CH, ²J_{AB} = 13.3 Hz), 3.37 (d, 3H, benzylic CH, ²J_{AB} = 15.0 Hz), 4.23 (d, 3H, benzylic CH, ²J_{AB} = 15.0 Hz), 6.82 (d, 3H, ring H(3), ³J = 9.7 Hz), 7.56 (s, 3H, ring H(6)), 7.68 (d, 3H, ring H(4), ³J = 9.7 Hz) ppm. ⁷¹Ga NMR (D₂O, pD = 9.3): δ = +34 ppm, W_{1/2} = 3400 Hz.

Na₃[In(TAMS)]. ¹H NMR (300 MHz, D₂O, pD = 9.7): 0.70 (s, 3H, methyl CH₃), 2.76 (d, 3H, methylenic CH, ²J_{AB} = 15.0 Hz), 2.90 (d, 3H, methylenic CH, ²J_{AB} = 15.0 Hz), 3.57 (d, 3H, benzylic CH, ²J_{AB} = 14.3 Hz), 4.08 (d, 3H, benzylic CH, ²J_{AB} = 15.0 Hz), 6.62 (d, 3H, ring H(3), ³J = 8.7 Hz), 7.49 (d, 3H, ring H(6), ⁴J = 2.3 Hz), 7.63 (dd, 3H, ring H(4), ³J = 8.7 Hz, ⁴J = 2.3 Hz) ppm. ¹¹⁵In NMR (D₂O, pD = 9.7): δ = +113 ppm, W_{1/2} = 26 000 Hz.

Na₃[Al(TAPS)]. ¹H NMR (200 MHz, D₂O, pD = 9.0): 2.52 (d, 1H, methylenic CH, ²J_{AB} = 13 Hz), 2.86 (d, 1H, methylenic CH', ²J_{AB} = 13 Hz), 3.05 (s, 1H, methine CH), 3.36 (d, 1H, methylenic CH, ²J_{AB} = 13 Hz), 3.48 (d, 1H, benzylic CH, ²J_{AB} = 13 Hz), 3.53 (d, 1H, benzylic CH', ²J_{AB} = 13 Hz), 3.73 (d, 1H, methylenic CH', ²J_{AB} = 13 Hz), 3.77 (d, 1H, benzylic CH, ²J_{AB} = 13 Hz), 3.93 (d, 1H, benzylic CH'', ²J_{AB} = 13 Hz), 4.24 (d, 1H, benzylic CH'', ²J_{AB} = 13 Hz), 4.35 (d, 1H, benzylic CH', ²J_{AB} = 13 Hz), 5.91 (d, 1H, ring H(3), ³J = 8.8 Hz), 6.82 (d, 1H, ring H(3'), ³J = 8.5 Hz), 6.98 (d, 1H, ring H(3''), ³J = 8.5 Hz), 7.38 (d, 1H, ring H(6'), ⁴J = 2.0 Hz), 7.39 (dd, 1H, ring H(4), ³J = 8.5 Hz, ⁴J = 2.0 Hz), 7.49 (d, 1H, ring H(6), ⁴J = 2.0 Hz), 7.57 (d, 1H, ring H(6''), ⁴J = 2.0 Hz), 7.65 (dd, 1H, ring H(4'), ³J = 8.5 Hz, ⁴J = 2.0 Hz), 7.67 (dd, 1H, ring H(4''), ³J = 8.5 Hz, ⁴J = 2.0 Hz) ppm. ²⁷Al NMR (D₂O, pD = 9.0): δ = +16 ppm, W_{1/2} = 660 Hz.

Na₃[Ga(TAPS)]. ¹H NMR (200 MHz, D₂O, pD = 9.4): 2.53 (d, 1H, methylenic CH, ²J_{AB} = 13 Hz), 2.94 (d, 1H, methylenic CH', ²J_{AB} = 13 Hz), 3.07 (s, 1H, methine CH), 3.46 (d, 1H, methylenic CH, ²J_{AB} = 13 Hz), 3.50 (d, 1H, benzylic CH, ²J_{AB} = 13 Hz), 3.57 (d, 1H, benzylic CH', ²J_{AB} = 13 Hz), 3.76 (d, 1H, methylenic CH', ²J_{AB} = 13 Hz), 3.76 (d, 1H, benzylic CH, ²J_{AB} = 13 Hz), 3.97 (d, 1H, benzylic CH'', ²J_{AB} = 13 Hz), 4.33 (d, 1H, benzylic CH'', ²J_{AB} = 13 Hz), 4.43 (d, 1H, benzylic CH', ²J_{AB} = 13 Hz), 5.81 (d, 1H, ring H(3), ³J = 8.5

Hz), 6.88 (d, 1H, ring H(3'), $^3J = 8.5$ Hz), 7.02 (d, 1H, ring H(3''), $^3J = 8.5$ Hz), 7.38 (d, 1H, ring H(6), $^4J = 2.0$ Hz), 7.40 (dd, 1H, ring H(4), $^3J = 8.5$ Hz, $^4J = 2.0$ Hz), 7.48 (d, 1H, ring H(6'), $^4J = 2.0$ Hz), 7.58 (d, 1H, ring H(6''), $^4J = 2.0$ Hz), 7.66 (dd, 1H, ring H(4'), $^3J = 8.5$ Hz, $^4J = 2.0$ Hz), 7.68 (dd, 1H, ring H(4''), $^3J = 8.5$ Hz, $^4J = 2.0$ Hz) ppm. ^{71}Ga NMR (D_2O , pD = 9.4): $\delta = +57$ ppm, $W_{1/2} = 1230$ Hz.

$\text{Na}_3[\text{In}(\text{TAPS})]$. ^1H NMR (200 MHz, D_2O , pD = 9.6): 2.62 (d, 1H, methylenic CH), 3.03 (d, 1H, methylenic CH'), 3.11 (s, 1H, methine CH), 3.50 (d, 1H, benzylic CH), 3.61 (d, 1H, methylenic CH), 3.61 (d, 1H, benzylic CH'), 3.74 (d, 1H, methylenic CH'), 3.83 (d, 1H, benzylic CH), 3.94 (d, 1H, benzylic CH'), 4.41 (d, 1H, benzylic CH'), 4.41 (d, 1H, benzylic CH'), 6.09 (d, 1H, ring H(3), $^3J = 8.5$ Hz), 6.99 (d, 1H, ring H(3'), $^3J = 8.6$ Hz), 7.05 (d, 1H, ring H(3''), $^3J = 8.6$ Hz), 7.37 (d, 1H, ring H(6), $^4J = 2.4$ Hz), 7.42 (dd, 1H, ring H(4), $^3J = 8.5$ Hz, $^4J = 2.4$ Hz), 7.62 (d, 1H, ring H(6'), $^4J = 2.3$ Hz), 7.62 (d, 1H, ring H(6''), $^4J = 2.3$ Hz), 7.68 (dd, 1H, ring H(4'), $^3J = 8.6$ Hz, $^4J = 2.3$ Hz), 7.68 (dd, 1H, ring H(4''), $^3J = 8.6$ Hz, $^4J = 2.3$ Hz) ppm. ^{115}In NMR (D_2O , pD = 9.6): $\delta = +175$ ppm, $W_{1/2} = 22\,000$ Hz.

$\text{Na}_3[\text{Ga}(\text{TRNS})]$. ^{13}C NMR (75.5 MHz, D_2O , pD = 10.0): 42.14, 42.81, 43.06, 44.02, 46.01, 48.54, 48.81, 50.96, 51.14, 51.69, 52.00, 52.25, 55.43, 55.61, 57.74, 119.30, 119.55, 120.27, 120.83, 120.97, 123.46, 127.25, 127.49, 127.60, 127.82, 128.16, 128.54, 128.99, 130.57, 131.82, 165.11, 165.77 ppm.

$\text{Na}_3[\text{In}(\text{TRNS})]$. ^1H NMR (300 MHz, D_2O , pD = 9.0): 2.55 (m, 6H, ethylene CH_2), 3.62 (d, 3H, benzylic CH, $^2J_{\text{AB}} = 11.4$ Hz), 5.08 (d, 3H, benzylic CH, $^2J_{\text{AB}} = 11.4$ Hz), 6.87 (d, 3H, ring H(3), $^3J = 8.1$ Hz), 7.57 (d, 3H, ring H(6), $^4J = 2.4$ Hz), 7.64 (dd, 3H, ring H(4), $^3J = 8.1$ Hz, $^4J = 2.4$ Hz) ppm.

$\text{Na}_3[\text{Ga}(\text{TACS})]$. Four equivalents of $\text{Ga}(\text{NO}_3)_3$ were added to a H_6TACS solution at pD = 9.3, and the solution was heated to 70 °C for 30 min. A white solid was filtered off, and the ^1H and ^{71}Ga NMR spectra were obtained for the filtrate. The filtrate was found to contain about 70% complex and 30% unreacted ligand. ^1H NMR (300 MHz, D_2O , pD = 9.3, see Scheme 4): 1.92 (d, 3H, H(A_{ax}), $^2J_{\text{AB}} = 15$ Hz), 2.34 (d, 3H, H(B_{eq}), $^2J_{\text{AB}} = 15$ Hz), 3.28 (s, 3H, H(C_{eq})), 3.76 (d, 3H, benzylic CH, $^2J_{\text{AB}} = 12.8$ Hz), 4.07 (d, 3H, benzylic CH, $^2J_{\text{AB}} = 12.8$ Hz), 6.41 (d, 3H, ring H(3), $^3J = 8$ Hz), 7.56 (d, 3H, ring H(6), $^4J = 2.4$ Hz), 7.60 (dd, 3H, ring H(4), $^3J = 8$ Hz, $^4J = 2.4$ Hz) ppm. ^{71}Ga NMR (D_2O , pD = 9.3): $\delta = +18$ ppm, $W_{1/2} = 1000$ Hz.

Potentiometric Equilibrium Measurements. The equilibrium constants were determined by potentiometric methods as described previously.²⁹ The ionic strength was fixed at 0.16 M NaCl, and the solutions were maintained at 25 °C. Argon, which had been passed through 10% NaOH, was bubbled through the solutions to exclude CO_2 .

The ligand was checked for purity by NMR and elemental analysis before titration. Titrations were also employed to verify the molecular weight obtained by elemental analysis. Fresh ligand solutions were used as the ligands slowly oxidize in aerated solutions, especially in the presence of base. The metal ion solutions were prepared by dilution of the appropriate atomic absorption (AA) standards. The exact amount of acid present in the AA standards was determined by titration of an equimolar solution of metal standard and $\text{Na}_2\text{H}_2\text{EDTA}$. The amount of acid present was determined by Gran's method,³⁰ and this is equal to the amount of acid in the AA standard plus the 2 equiv of acid that were liberated from the complexed EDTA.

The ratio of ligand to metal used was $1:1 < \text{L}:\text{M} < 3:1$. Concentrations were in the range 0.5–2.5 mM. A minimum of five titrations were performed for each metal–ligand combination, each titration consisting of about 100 data points. The ligand solutions were titrated over the range $2 < \text{pH} < 11.5$, while the metal–ligand solutions were titrated over the range 2–11. Complexation was usually rapid (1–3 min per point to give a stable pH reading) in the Ga(III) and In(III) studies; however, caution was taken to ensure that no trace hydrolysis or precipitation was occurring by monitoring up to 30 min for pH drift.

For the Al(III) stability constant studies, and for those involving Ga(III) with H_6TACS , equilibration was too slow for the automated

titration procedure and a batch method was employed instead. Here, a series of 24 (0.16 M NaCl) CO_2 -free solutions was prepared with a 1.1:1 L:M ratio, and varying amounts of NaOH were added. These solutions were equilibrated at 25 °C until the pH reading of each stabilized. Two batches of titrations were performed for Al–TAMS and Al–TAPS, and these titrations were fully equilibrated within 3 days. For Ga–TACS, equilibrium was not reached after five weeks, and TACS could not prevent some degree of $\text{Ga}(\text{OH})_3$ formation even after standing for 3 months. Any solutions containing precipitate were excluded from the refinement of data.

The data were refined using the program BEST.³¹ The hydrolysis constants used were taken from Baes and Mesmer,³² and in the case of In(III), formation constants with chloride were also included in the model. The data was modeled initially with only a ML species. To this simple model was added protonated species, H_2ML , or hydroxo species, $\text{ML}(\text{OH})$, sequentially. All of the metal complex equilibria could be explained satisfactorily with ML and sometimes HML; the inclusion of other species only worsened the fit.

Results and Discussion

Ligand Syntheses. Evans and Jukobovic^{16,17} have previously reported on the Al, Ga, In, and Fe complexes of saltrens and saltames; however, they prepared these complexes *in situ*, by a template method, and they never did isolate the free ligands. The Schiff bases reported here are all easily prepared by mixing the appropriate amine with sodium 5-sulfosalicylaldehyde in methanol. Although these compounds hydrolyze readily in water, they are stable in deuterated DMSO for weeks.

The Schiff bases are isolated as trisodium salts as evinced by their mass spectra which give the parent ion in a pattern that is typical of three sodium atoms being present, *i.e.*, $[\text{M} - 3\text{Na} + 4\text{H}]^+$, $[\text{M} - 2\text{Na} + 3\text{H}]^+$, ..., $[\text{M} + \text{Na}]^+$. The sulfonated amine phenols are all isolated as inner salts. Positive LSIMS shows the parent ion plus one, and the elemental analyses are in agreement with the proposed formulations; there is no evidence for a sodium salt. The NMR spectra of these compounds are straightforward owing to the 2- or 3-fold symmetry present in the molecules. Loss of the imine NMR resonances at 8.7 (^1H) and 166 ppm (^{13}C) and the appearance of benzylic resonances at ca. 3.6 (^1H) and 55 ppm (^{13}C) are diagnostic of the proposed formulations.

The infrared spectra of these four Schiff bases were about 90% superimposable, indicating the dominance of the 2-hydroxy-5-sulfonatobenzylidene moiety on the spectra; likewise, the series of amine phenols had virtually superimposable IR spectra. The most dramatic difference between an amine phenol and its corresponding Schiff base was the exceedingly broad absorption between 3500 and 2600 cm^{-1} in the amine phenols, indicative of extensive hydrogen bonding in the solids; with the Schiff bases, there existed only a 50 cm^{-1} wide band centered at 3450 cm^{-1} . The loss of the imine linkage was also detected by IR, where the $\text{C}=\text{N}$ stretch at 1640 cm^{-1} is replaced by an $\text{N}-\text{H}$ bend at 1605 cm^{-1} after treatment of the Schiff base with borohydride.

Deprotonation Constants and Conformational Changes. The pK_{a} s of the four amine phenols that were treated here all showed similar behavior. The three phenolate moieties in each had pK_{a} s between 6 and 9, demonstrated in Figure 1 where the molar absorptivity at 256 nm is plotted against pH. Since the phenolic group is the only significant chromophore in each molecule, any change in the UV spectrum is attributable to phenol deprotonation—a bathochromic shift in the absorption bands (232 → 256 nm, 276 → 288 nm) and a concomitant

(29) Caravan, P.; Hédlund, T.; Liu, S.; Sjöberg, S.; Orvig, C. *J. Am. Chem. Soc.* **1995**, *117*, 11230.

(30) Gran, G. *Acta Chem. Scand.* **1950**, *4*, 559.

(31) Motekaitis, R. J.; Martell, A. E. *Can. J. Chem.* **1982**, *60*, 2403.

(32) Baes, C. F., Jr.; Mesmer, R. E. *Hydrolysis of Cations*; Wiley-Interscience: New York, 1976.

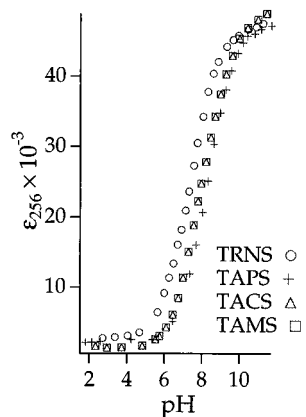


Figure 1. Plot of molar absorptivity at 256 nm vs pH for H_6TRNS , H_6TAPS , H_6TACS , and H_6TAMS .

Table 1. Deprotonation Constants (0.16 M NaCl, 25 °C)^a

	pK_a							
	H_6TRNS		H_6TAMS		H_6TAPS^b		H_6TACS	
1	11.2(1)	N-H	11.19(4)	N-H	11.24(9)	N_o -H	11.24(5)	N-H
2	10.6(1)	N-H	9.81(4)	N-H	9.77(6)	N_o -H	9.84(2)	N-H
3	9.59(3)	N-H	8.91(2)	O-H	8.73(4)	O_i -H	8.95(1)	O-H
4	8.07(3)	O-H	7.95(3)	O-H	7.78(3)	O_o -H	7.85(2)	O-H
5	7.29(3)	O-H	6.56(2)	O-H	6.54(2)	O_o -H	7.08(1)	O-H
6	6.17(3)	O-H	2.92(2)	N-H	1.7(1)	N_i -H	6.01(3)	N-H

^a The numbers in parentheses refer to 1σ . N-H and O-H refer to ammonium and phenol deprotonation, respectively. ^b The subscripts o and i refer to the outer and inner arms, respectively.

increase in ϵ_{max} .³³ The band at 256 nm was monitored, since this undergoes the largest change versus pH; however, graphs with the same pH profile can be generated from other wavelengths between 200 and 300 nm.

Variable pD 1H NMR can also be used to probe the deprotonation of the ligands. In H_6TAMS , H_6TAPS , and H_6TACS , the first deprotonation occurred at an ammonium center, whereas in H_6TRNS , the first deprotonation was a phenol. Comparison of the deprotonation constants for the parent amines tame, tap, tach, and tren gives a useful empirical relationship. If the amine has a $pK_a < 8$ then this pK_a becomes lower in the amine phenol, whereas a $pK_a > 8$ in the parent amine becomes elevated in the corresponding amine phenol.

Because H_6TAPS lacks the 3-fold symmetry of the other molecules, more information can be gleaned about its deprotonation. The central arm of H_6TAPS is distinguishable from the outer arms, and this allows the assignments of the pK_a s in Table 1. Figure 2 shows the influence of pH on the chemical shift of various 1H resonances in H_6TAPS ; it is clear from the benzylic and the amine backbone shifts (parts a and b of Figure 2) that the inner arm ammonium is the first site to deprotonate. The shift of the ring H(3) (Figure 2c) indicates that the outer arm phenol moieties deprotonate first, followed by the inner phenol moiety. This deprotonation scheme is expected since the inner amine offers a site to hydrogen bond to the inner phenol, and this should raise the pK_a of the inner phenol group, relative to the outer phenol groups.

Somewhat surprising behavior was noted for the benzylic, methylene backbone, and methine backbone resonances, especially when the molecule was in the protonation state H_5TAPS^- (Figure 3 shows the 1H NMR at various pD). When the molecule is hexaprotonated (pD = 0.9), the two benzylic peaks

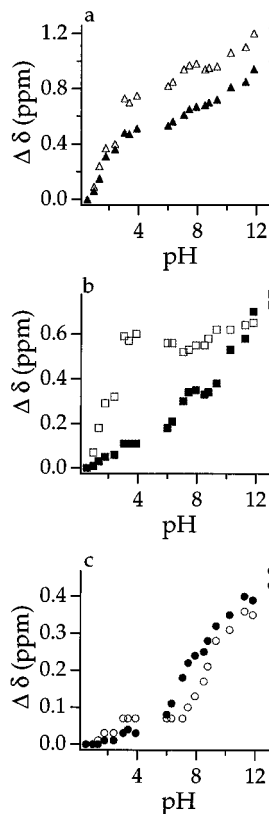


Figure 2. Plot of change in 1H chemical shift vs pH for (a) benzylic, (b) amine backbone, and (c) ring H(3) protons of H_6TAPS . Filled symbols correspond to outer arms and open symbols to inner arm.

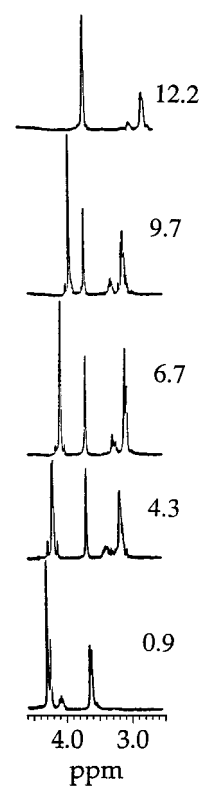


Figure 3. Aliphatic and benzylic portion of 1H NMR spectra of H_6TAPS at various pD.

almost overlap and are seen as sharp singlets (δ 4.35, 4.30). The methine resonance is the expected quintet (δ 4.13), while the methylene peak appears as a doublet (δ 3.66). Raising the pD to 4.3 reveals that the outer benzylic peak (δ 4.24) is split into an AB doublet ($^2J_{AB} = -12.9$ Hz), while the inner benzylic

(33) Silverstein, R. M.; Bassler, G. C.; Morrill, T. C. *Spectrometric Identification of Organic Compounds*, 4th ed.; Wiley: New York, 1981.

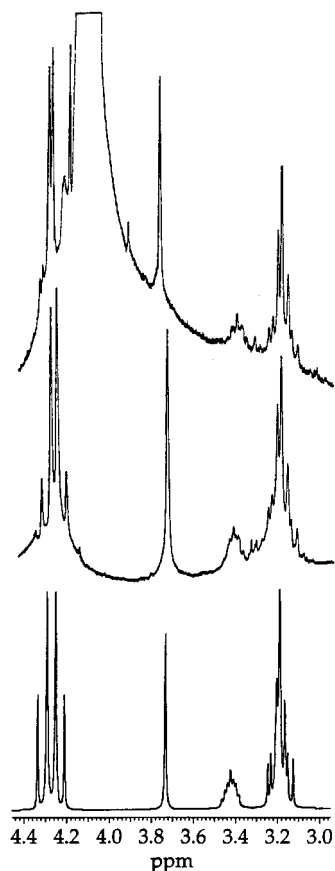


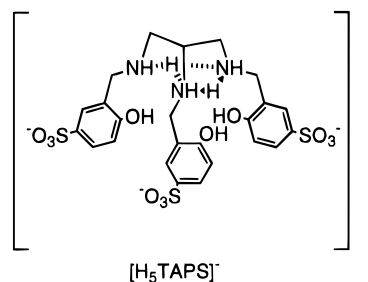
Figure 4. Aliphatic and benzylic portion of ^1H NMR spectra of $\text{H}_6\text{-TAPS}$ at $\text{pD} = 4.3$: bottom (25°C , simulated), middle (25°C), top (85°C).

resonance (δ 3.70) remains a sharp singlet. The methine (δ 3.38) and methylene (δ 3.15) signals now form a complex multiplet of an $\text{AA}'\text{BB}'\text{C}$ spin system ($^2J_{\text{AB}} = ^2J_{\text{A'B'}} = -12$ Hz, $^3J_{\text{AC}} = ^3J_{\text{A'C}} = 8$ Hz, $^3J_{\text{BC}} = ^3J_{\text{B'C}} = 4$ Hz). Upon deprotonation of a phenol group ($\text{pD} = 6.7$), the spectrum once again simplifies and the methylene hydrogen atoms are once more seen as a doublet. When all three phenol moieties are deprotonated ($\text{pD} = 9.7$), there is again evidence for rigidity. In this instance, the methylene resonance shows the same splitting pattern as in the $\text{pD} = 4.3$ spectrum, but now the benzylic resonances are both singlets. At the point of complete deprotonation ($\text{pD} = 12.2$), the spectrum is again simplified. Here, the benzyl resonances overlap, and the methylene resonance is once again a doublet.

To examine further this behavior, the sample at $\text{pD} = 4.3$ was heated in 15°C increments to 85°C . The only change in the 85°C spectrum was the migration of the HOD peak to overlap the benzylic AB quartet. Figure 4 shows the spectrum of the $\text{pD} = 4.3$ sample at 25°C (middle), its simulation using the coupling constants listed in the previous paragraph (bottom), and the sample at 85°C (top). At 85°C , the HOD resonance has shifted to lower frequency such that the outer arm benzyl resonance can once again be seen. There is very little change between the 85 and 25°C spectra. The separation of the outer arm A and B benzyl resonances decreases slightly at the higher temperature, and the inner arm benzylic hydrogen atom resonance shifts slightly to a higher frequency. However, the massive HOD resonance occurring in the 85°C spectrum makes phasing difficult, and quantitation of small shift changes is obviated. There are some minor resonances located about 3.3 ppm in the 25°C spectrum that are not present in the simulation. These could be either an impurity or a minor conformer. A

minor conformer would be expected to have a temperature dependence on its intensity if there is a conformational equilibrium. There is such a change, which suggests the presence of a minor conformer, and the minor conformer appears to be disfavored at higher temperatures.

These observations lead to the proposal of a conformation of H_5TAPS^- as shown below. Deprotonation of the inner arm



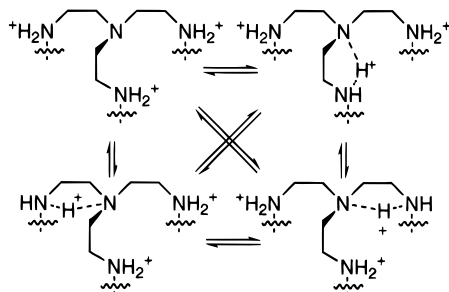
ammonium leads to the formation of a hydrogen bond network of three hydrogen bonds among the three nitrogen atoms giving rise to one six-membered and two five-membered rings, whereby the outer arm ammonium nitrogen atoms share their hydrogen atoms with the inner arm amine nitrogen atom. Such a solution structure would explain the ^1H NMR spectrum, which still shows 2-fold symmetry. The inner arm benzylic resonance appears as a singlet since both hydrogen atoms point toward an outer arm benzylic hydrogen atom. The outer arm benzylic carbon atoms have one attached hydrogen atom facing toward the inner arm benzyl group, while the second hydrogen atom faces toward the other outer arm benzyl group; this would give the observed AB quartet. This is also consistent with the $\text{AA}'\text{BB}'\text{C}$ pattern that is seen for the backbone and the coincidence of the chemical shifts of $\delta_{\text{A}} = \delta_{\text{A}'}$ and $\delta_{\text{B}} = \delta_{\text{B}'}$.

Loss of another proton, this time from an outer arm phenol, to give $\text{H}_4\text{TAPS}^{2-}$ leads to singlets for both of the benzylic resonances and a doublet for the methylene group (Figure 3, $\text{pD} = 6.7$). Presumably, this is because of more than one hydrogen bonding network available to the molecule, and these hydrogen bonding arrangements are close in energy. For instance, in addition to the arrangement shown above (with a phenol deprotonated now), there should be a strong charged hydrogen bond available between the phenolate oxygen atom and the outer arm ammonium. This is also available to the second outer arm ammonium, and rapid conversion between the three would account for the spectrum shown in Figure 3. As the molecule is successively deprotonated, more arrangements exist for the formation of intramolecular hydrogen bonds, and this eliminates the presence of one rigid solution structure.

The presence of this strong intramolecular hydrogen bonding which remains intact at 85°C in H_2O argues strongly for the preorganized nature of $\text{H}_x\text{TAPS}^{n-}$ in intermediate states of deprotonation. This should contribute a favorable entropy for the complexation of metal ions. A similar effect should exist with H_6TRNS . The apical nitrogen atom is known to be very acidic ($\text{pK}_{\text{a}} < 1.5$);^{29,34} therefore, there is the possibility of the four nitrogen atoms sharing the three hydrogen atoms through a series of alternating hydrogen bonds involving the secondary and tertiary nitrogen atoms (Scheme 5). A similar process can be envisaged for H_5TAMS^- , since the first pK_{a} of H_6TAMS (2.91) is also quite acidic; however, because both $\text{H}_x\text{TRNS}^{n-}$ and $\text{H}_x\text{TAMS}^{n-}$ possess 3-fold symmetry, the benzylic, ethylenic, or methylenic H atoms will always appear equivalent, and the presence of this effect cannot be confirmed by ^1H NMR.

(34) Galdes, C. F. G. C.; Brücher, E.; Cortes, S.; Koenig, S. H.; Sherry, A. D. *J. Chem. Soc., Dalton Trans.* **1992**, 2517.

Scheme 5



The high acidity of an amino group in the three molecules discussed above can be thought of in two ways. Firstly, the protonation of all of the amino groups would result in a large local charge increase, and the ease of proton loss is a result of the reducing coulombic repulsion. Secondly, the deprotonated molecule may also exhibit added stability because of the possibility of the formation of hydrogen bonds between an ammonium group and a neighboring amine. If this occurs (and the ^1H NMR of H_5TAPS^- supports this), then these molecules can exhibit some degree of preorganization in forming a tripodal cavity.

H_6TACS undergoes a considerably different protonation behavior when compared with the three compounds discussed above. Both the parent amine tach and the amine phenol described here exist in the equatorial conformation, in which the amino groups point away from each other. This is clearly delineated by the coupling constants that are obtained for the three distinct cyclohexane ring hydrogen atoms (H_A , H_B , H_C). In Scheme 4, the two possible conformers and their respective Newman projections are presented. If the equatorial conformer obtains, the methine hydrogen (H_C) should exhibit a large (8–12 Hz) vicinal coupling to the axial hydrogen atom (H_A) and an intermediate (2–4 Hz) vicinal coupling to the equatorial hydrogen atom (H_B).³⁵ An axial conformation would give coupling constants in the range $^3J_{AC} = 2\text{--}4$ Hz and $^3J_{AB} = 1\text{--}3$ Hz.³⁵ The observed constants are $^3J_{AC} = 11.7$ Hz and $^3J_{AB} = 2$ Hz, confirming the equatorial conformer. This is expected since the parent amine tach²⁷ and the Schiff base saltachs (*vide supra*) both exist in the equatorial conformation. The difference in energy between the axial and equatorial conformers for tach has been calculated to be 11 kcal/mol in the gas phase,³⁶ and this has been confirmed in a recent MM3 study.³⁷ The equatorial conformer of the amine phenol H_6TACS , because of the steric bulk of the benzyl groups, should be even more stable relative to the axial conformer. The equatorial conformer is present over the pH range studied in the ^1H NMR titration (pD = 1–13). A pD = 12 solution was heated to 90 °C with no change observed.

The equatorial conformation has ramifications in the magnitude of the pK_a s of H_6TACS . The first deprotonation occurs at one of the ammonium moieties, but this ammonium is considerably less acidic ($\text{pK}_a = 6$) than the analogous H_6TAMS ($\text{pK}_a = 2.9$) ammonium. This is because the physical separation of the ammonium groups is greater than that in H_6TAMS and also because the deprotonated species H_5TACS^- has no opportunity to form an intramolecular hydrogen bond between an amine and ammonium group. The higher basicity of this ligand, compared to TAMS^{6-} or TAPS^{6-} , manifests itself in the ability to bind metal ions in acidic media (*vide infra*).

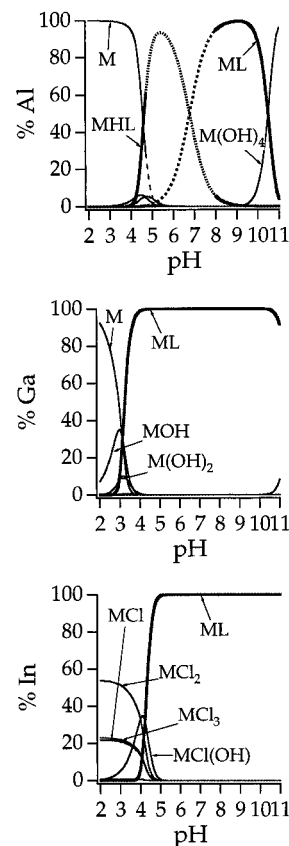


Figure 5. Speciation diagram of 2 mM M(III) ($\text{M} = \text{Al, Ga, In}$)/2 mM H_6TAMS . Dashed lines indicate the region where precipitation occurs (charges omitted for simplicity).

Since metal complexes of TACS derivatives must have the ligand in an axial conformation, complexation must involve a ring-flip. No evidence of conformational interconversion was observed in the uncomplexed ligand at 90 °C. This kinetic barrier to conformational change, coupled with the fact that the axial conformer is higher in energy than the equatorial conformer, results in slow metal complexation kinetics (*vide infra*).

Metal Complexes. $\text{M(III)}\text{--TAMS}$. The most straightforward complexation reactions were those involving H_6TAMS . The gallium(III) and indium(III) complexes formed rapidly (1–2 min per data point) and were completely formed by pH 4 and 5, respectively. The aluminum(III) complex formed slowly, necessitating a batch titration method. With $[\text{Al}(\text{TAMS})]^{3-}$, pH readings were stable after 1 day; however, the stability of the aluminum complex was insufficient to prevent some precipitation of $\text{Al}(\text{OH})_3$. Ga(III) and In(III) only form $[\text{M}(\text{TAMS})]^{3-}$ complexes, whereas Al(III) forms this species as well as a $[\text{M}(\text{HTAMS})]^{2-}$ species. The most stable species here is $[\text{Ga}(\text{TAMS})]^{3-}$, and this is clearly seen in the speciation diagram (Figure 5) which compares the complexation behavior of TAMS^{6-} with the three metals. Notably, Al(III) complexation begins at about the same pH as for In(III) , because of the formation of the protonated Al complex; however, $[\text{Al}(\text{TAMS})]^{3-}$ is much less stable than is $[\text{In}(\text{TAMS})]^{3-}$, and this leads to some precipitation of $\text{Al}(\text{OH})_3$ (the region where $\text{Al}(\text{OH})_3$ coexists is denoted by dashed lines). Another point to note from the speciation diagrams is the formation of chloro complexes of indium. Using an ionic medium of sodium chloride gives rise to chloro complexes at low pH, and the formation of these species suppresses the formation of $\text{In}(\text{OH})_3$. The result is a larger experimental window (about one pH unit) for the determination of indium stability constants. Use of nitrate or perchlorate as a background electrolyte would have introduced

(35) Abraham, R. J.; Gatti, G. J. *J. Chem. Soc. B* **1969**, 961.

(36) Childers, R. F.; Wentworth, R. A. D.; Zompa, L. J. *Inorg. Chem.* **1971**, *10*, 302.

(37) Ivery, M.; Weiler, L. S. Unpublished results.

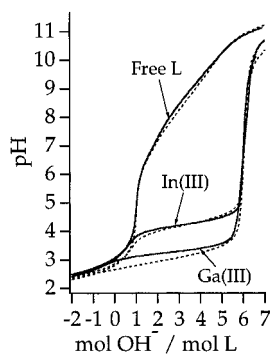


Figure 6. Experimental titration curves for 2 mM M(III) (M = Ga, In)/2 mM H₆L. Dashed lines represent H₆TAPS titrations, solid lines represent H₆TAMS.

Table 2. Metal–Ligand Formation Constants (0.16 M NaCl, 25 °C)

	log K		
	Al(III)	Ga(III)	In(III)
M(HTRNS) ²⁻		36.90(7)	34.9(1)
M(TRNS) ³⁻		28.55(5)	29.3(1)
M(HTAMS) ²⁻	29.3(1)		
M(TAMS) ³⁻	22.5(1)	31.83(5)	28.49(3)
M(HTAPS) ²⁻	29.0(1)	35.15(4)	31.93(4)
M(TAPS) ³⁻	22.8(1)	31.54(4)	27.56(4)

complications because of the competition of In(OH)₃ formation during the titrations.

The ¹H NMR spectra of the TAMS complexes are similar; the Al, Ga, and In complexes all show the expected 3-fold symmetry in solution. Furthermore, the complexes are rigid in solution, as evinced by the inequivalence of the two benzylic hydrogen atoms and the inequivalence of the two methylene hydrogen atoms. This is analogous to the spectra observed in the nonsulfonated complexes,²¹ which were obtained in DMSO-*d*₆. In the [M(TAMS)]³⁻ complexes, the chemical shift separation of the methylene AB doublets increased down the the group (Al vs Ga vs In), whereas the chemical shift separation of the benzylic AB doublets decreased down the same group. This is likely a size effect (observed and discussed previously in the solid state structures of the nonsulfonated analogs²¹) which results in a change in the torsion angles about the benzylic and methylene carbon atoms.

M(III)–TAPS. The stability constants of the [M(TAPS)]³⁻ complexes were of the same order of magnitude as those of their analogous TAMS complexes, but were slightly less in the actual value (Table 2). In addition, all three metals formed stable protonated complexes. Again, a batch titration was necessary to determine the Al binding constants, and as with TAMS, TAPS⁶⁻ was unable to prevent some degree of aluminum hydroxide formation. This is in accord with the observations of Liu *et al.*^{20,21} who noted that it was difficult to prepare analytically pure samples of the Al(III) complexes of the unsulfonated TAMS and TAPS analogs without some occlusion of Al(OH)₃. Figure 6 shows experimental 1:1 M/L titration curves for Ga(III) and In(III) along with curves for the free ligands, H₆TAMS and H₆TAPS. The coincidence of each pair of curves shows the similar binding ability of the two ligands. Although the stability constant of [Ga(TAPS)]³⁻ is slightly less than that of [Ga(TAMS)]³⁻, the formation of the protonated species [Ga(HTAPS)]²⁻ enables Ga sequestration at a lower pH.

The ¹H NMR of the [M(TAPS)]³⁻ complexes were similar to each other and to those reported for nonsulfonated analogs.²⁰ All three arms are inequivalent in the complexes, giving rise to

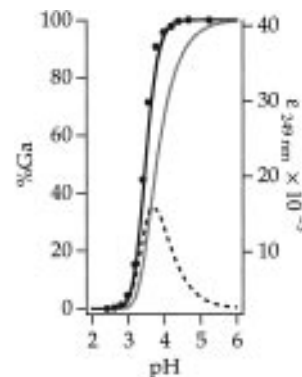


Figure 7. Partial speciation diagram ([Ga(OH)₃]^{(3-x)+} species omitted for clarity) for 1 Ga(III):1 H₆TAPS (30 μM) and the absorbance at 249 nm vs pH: [Ga(HTAPS)]²⁻ (---), [Ga(TAPS)]³⁻ (···), ([Ga(HTAPS)]²⁻ + [Ga(TAPS)]³⁻) (—●), ε at 249 nm (●).

20 distinct resonances. ¹H–¹H COSY experiments allow partial assignment of the spectra. One striking feature of the ¹H NMR spectra of the [M(TAPS)]³⁻ complexes is the resonance of the ring 3' hydrogen (H(3) *ortho* to the oxy group). Two of the three arms have resonances in the chemical shift range of the other coordinated phenolates in this study (6.6–7.1 ppm), but the third arm is significantly deshielded, resonating between 5.9 and 6.1 ppm in the Al, Ga, and In complexes. Examination of the 5'-methoxy substituted Ga complex, as well as models of the complexes in this work, suggest that this is one of the outer arms.

¹H NMR was used to probe the solution structure of [Ga(HTAPS)]²⁻, but since this species is always in equilibrium with free H₅TAPS⁻ and/or [Ga(TAPS)]³⁻, the observed spectrum was a series of overlapping peaks. A Ga–TAPS UV pH titration was carried out in another effort to elucidate the coordination sphere of [Ga(HTAPS)]²⁻. In the H_xTAPSⁿ⁻ system, the protonated phenols have an absorption maximum at 232 nm; upon deprotonation to the phenolate anion, this maximum shifts to 256 nm. Titration of a 1.1:1 Ga/TAPS solution saw the appearance of a new band at 249 nm, assignable to the coordination of a phenolato group to gallium. Figure 7 shows a partial speciation diagram (only the Ga–TAPS species are shown for simplification), along with the absorbance at 249 nm as a function of pH. The [Ga(HTAPS)]²⁻ species can have an N₃O₂ or an N₂O₃ donor set from the ligand, or both cases can exist if there is more than one isomer. The rise in absorbance mirrors exactly the curve for the formation of [Ga(HTAPS)]²⁻ + [Ga(TAPS)]³⁻, suggesting that [Ga(HTAPS)]²⁻ has the ligand coordinated in an N₂O₃ manner, *i.e.*, with an amine still protonated. The change being monitored here is the extent of phenolate coordination. This change is complete when all of the ligand has been coordinated to Ga in one form or another ([Ga(HTAPS)]²⁻ + [Ga(TAPS)]³⁻). If the protonated species was an N₃O₂ isomer with a protonated phenol, one would expect to see a continued increase at 249 nm over another pH unit, until formation of [Ga(TAPS)]³⁻ is complete.

M(III)–TRNS. With H₆TRNS, the unsulfonated analogs showed diverse coordination chemistry (Scheme 2), with Al being coordinated by an N₃O₃ donor set, Ga by an N₄O₂ donor set, and In by an N₄O₃ donor set.¹⁸ Titrations of the Al–TRNS system yielded little useful information. There is no complexation up to pH 6 or above pH 10. UV titrations suggested that there may be some interaction between the phenolate groups and Al between pH 6 and 10. ¹H NMR titrations yielded spectra that were identical to the free ligand. If there is complexation, then exchange between [Al(H_xTRNS)]ⁿ⁻ and H_xTRNSⁿ⁻ is rapid. Any changes in the chemical shifts with respect to those

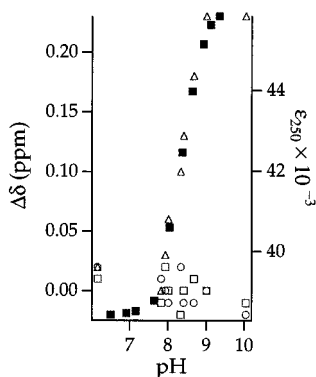
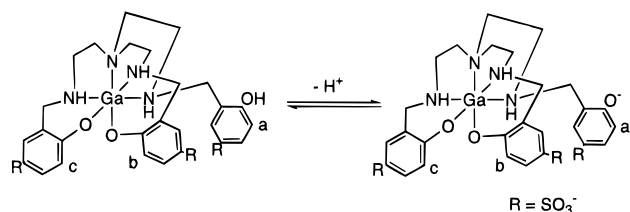


Figure 8. Plot of change in ^1H chemical shift (left axis) vs pH for the three ring H(3) hydrogen atoms (H(a) Δ , H(b) \circ , H(c) \square) as in Scheme 6) and plot of absorbance at 250 nm (right axis) vs pH (filled symbols) for $[\text{Ga}(\text{TRNS})]^{3-}$.

Scheme 6



in the free ligand were small (<0.04 ppm). Formation of $\text{Al}(\text{OH})_3$ obviated any potentiometric experiments.

Gallium complexation by TRNS was slower than that by TAMS or TAPS (5–10 min/pt). Two species were formed: a $[\text{Ga}(\text{HTRNS})]^{2-}$ complex which was 100% present at pH = 5.5 and a $[\text{Ga}(\text{TRNS})]^{3-}$ complex. ^1H NMR clearly demonstrated the lack of C_3 symmetry in solution—a series of overlapping signals were seen in the aliphatic, benzylic, and aromatic regions. The only region of the ^1H NMR spectrum that could be distinguished was between 6 and 7 ppm. In this region, three doublets corresponding to the 3' hydrogen atoms were observed. It was shown above (Figure 2c) and in previous work²⁹ that these resonances were sensitive to phenol deprotonation. Examination of a series of spectra (1:1 Ga/TRNS) showed only one of these doublets having a pH dependent chemical shift. In a UV titration, a plot of the change in absorbance at 250 nm, corresponding to phenol deprotonation, versus pH gave a sigmoidal curve. These results are summarized in Figure 8. This suggests that Ga is coordinated by an N_4O_2 donor set in the same manner as that observed in the crystal structure of the unsulfonated analog.¹⁸ The spectroscopic data clearly show that the deprotonation of $[\text{Ga}(\text{HTRNS})]^{2-}$ is taking place at a phenol. Since the chemical shifts of two of the 3' hydrogen atoms do not change, it is unlikely that this deprotonation involved a change in coordination geometry. Scheme 6 is a pictorial representation of the deprotonation process. The $\text{p}K_a$ value of 8.35 obtained from both the UV and NMR data is in accord with that obtained by potentiometry and is close to the value of the $\text{p}K_a$ of 4-sulfophenol (8.60).⁹ A ^{13}C NMR spectrum of the $[\text{Ga}(\text{TRNS})]^{3-}$ complex showed 26 of the expected 27 resonances (the 2' C region showed only 2 resonances, presumably because of overlap). This suggests that there is only one major ($>90\%$) isomer present.

The In–TRNS system was more straightforward. Equilibrium was established rapidly (1–2 min/pt) and TRNS complexed with In over the same pH range as it did with Ga. This is in contrast to the TAMS and TAPS systems where the Ga complexes were four orders of magnitude more stable than their In analogs. There is also a protonated species present,

$[\text{In}(\text{HTRNS})]^{2-}$, but it exists over a narrow pH range and never as the sole In-containing species. The ^1H NMR spectrum of $[\text{In}(\text{TRNS})]^{3-}$ is characteristic of a rigid complex (the benzylic H atoms are inequivalent) with 3-fold symmetry (only one set of resonances is observed for the three arms). The symmetry indicates that the donor set must be N_4O_3 or N_3O_3 with the apical nitrogen atom nonbonding. The former seven coordinate complex seems more likely. This was the case in the solid state structure of the unsulfonated analog.¹⁸ Coordination of the apical nitrogen should be favored because it results in the formation of three five-membered chelate rings. Also, $[\text{In}(\text{TRNS})]^{3-}$ should be more basic if there is an uncoordinated amine.

M(III)–TACS. No stability constants could be determined with H_6TACS because of its exceedingly slow kinetics with Al, Ga, and In. A batch titration with gallium did not equilibrate even over 1 month. During this period, a slight excess of TACS (1.1:1 TACS/Ga) could not prevent the precipitation (of some degree) of gallium hydroxide. There was evidence of complex formation, however. Using an excess of gallium (4 equiv) at a pD of 9.3 showed two species in the ^1H NMR. There was a 70:30 ratio of (presumably) $[\text{Ga}(\text{TACS})]^{3-}/\text{H}_x\text{TACS}^{n-}$. The Ga complex showed spectral similarities to similar nonsulfonated complexes reported by Roundhill and co-workers.²³ The gallium complex has the expected 3-fold symmetry in solution and also displays rigidity, as indicated by the inequivalence of the benzylic hydrogen atoms. The nitrogen donors of the ligand now occupy the axial positions of the cyclohexane ring, which is clear from the coupling constants. There was no evidence for an In–TACS complex utilizing the same preparative conditions.

The slow kinetics of complexation is undoubtedly because of the large energy barrier involved in the ring-flip conformational change (*vide supra*). Furthermore, because TACS is in the wrong conformation for binding, this will also be reflected in a greatly reduced thermodynamic binding constant.

Metal NMR. When possible, the metal NMR was recorded for the aforementioned complexes. ^{27}Al and ^{71}Ga are both quadrupolar nuclei ($I = 5/2$ and $3/2$, respectively) with sufficiently low quadrupole moments such that solution NMR can be recorded. Increasing the symmetry about the nuclei in question enables narrower line widths to be obtained. ^{71}Ga NMR spectra were obtained for all of the gallium complexes reported here with the exception of $[\text{Ga}(\text{TRNS})]^{3-}$. $[\text{Ga}(\text{TRNS})]^{3-}$ has an asymmetric N_4O_2 coordination geometry, whereas $[\text{Ga}(\text{TAMS})]^{3-}$, $[\text{Ga}(\text{TAPS})]^{3-}$, and $[\text{Ga}(\text{TACS})]^{3-}$ all have facial N_3O_3 coordination geometries. Using the same conditions employed for the N_3O_3 complexes ($[\text{Ga}] = 30$ mM, 10 000 pulses, 90° flip angle), no signal was observed for $[\text{Ga}(\text{TRNS})]^{3-}$, presumably because of the lowered N_4O_2 symmetry about the gallium center. $[\text{Ga}(\text{TAPS})]^{3-}$ resonated at +57 ppm relative to $\text{Ga}(\text{H}_2\text{O})_6^{3+}$ with $W_{1/2} = 1230$ Hz. The $[\text{Ga}(\text{TACS})]^{3-}$ resonance appeared at a lower frequency, +18 ppm ($W_{1/2} = 1000$ Hz); both of these spectra were acquired after 1000 pulses. $[\text{Ga}(\text{TAMS})]^{3-}$ displayed a markedly different behavior. It resonated at +34 ppm ($W_{1/2} = 3400$ Hz) and because of the broader line width required 10 000 pulses. A broadening of the line width is indicative of an exchange process, a change in the correlation time τ_c , or of lower symmetry about the metal ion.³⁸ There was no indication of intermolecular exchange in these complexes from their ^1H NMR spectra. Therefore, the broader line width observed for $[\text{Ga}(\text{TAMS})]^{3-}$ must be a result of a less symmetric environment about the gallium nucleus or an increase in τ_c . Examination of the crystal structures of the corresponding

unsulfonated Ga complexes^{20,21,23} shows that the [Ga(TAPS)]³⁻ analog suffers the greatest deviation from octahedral geometry. It has been observed that the ²⁷Al line widths in a series of tris(*N*-alkyl-3-oxy-4-pyridinonato)aluminum(III) complexes increased with increasing alkyl chain length, whereas the chemical shift remained static.³⁹ Likewise, Parker and co-workers noted in a ⁷¹Ga NMR study of 1,4,7-triazacyclononane-1,4,7-triyltrimethylenetris(alkylphosphinato)gallium(III) complexes that increasing the size of the alkyl group on the phosphorus atom increased the ⁷¹Ga line width.⁴⁰ Within each of these cases, the environment (electric field gradient) about the quadrupolar nuclei should be very similar and the line width change can be ascribed to a change in molecular tumbling. With [Ga(TAMS)]³⁻, the electric field gradient at the gallium nucleus should not be markedly different than in [Ga(TAPS)]³⁻ or [Ga(TACS)]³⁻; the greatest difference is in the overall shape of the complexes, and these shape differences will affect τ_c .

The chemical shifts for the gallium complexes lie in the range that is expected for octahedral gallium(III) complexes; Cole *et al.* have reported ⁷¹Ga chemical shifts for Ga in an N₃O₃ environment.⁴⁰ For a tris(amino)tris(carboxylato) environment, a shift of +171 ppm was observed, and this shifted to lower frequency, between +130 and +140 ppm when the carboxylate groups were replaced by substituted phosphinato groups. With three phenolates as oxygen donors, the chemical shift range moves to an even lower frequency.

The ²⁷Al NMR spectra of [Al(TAMS)]³⁻ and [Al(TAPS)]³⁻ followed the same trends as did their gallium congeners. Both appeared in the shift range that is expected for octahedral aluminum complexes. [Al(TAMS)]³⁻ resonated at a lower frequency than [Al(TAPS)]³⁻, and as in the gallium complex, it had a wider line width.

¹¹⁵In NMR were also recorded for [In(TAMS)]³⁻ and [In(TAPS)]³⁻; the line widths were outrageous (26 and 22 kHz, respectively). Despite this result, similar trends were observed—[In(TAMS)]³⁻ resonated to lower frequency than that of [In(TAPS)]³⁻ and again had a wider line width.

Comparisons with Other Multidentate Ligands. The *in situ* work of Evans and Jakubovic¹⁶ allows some comparisons to be made on the effect of changing from an imine to an amine nitrogen donor. In their studies on the group 13 complexes of saltames⁶⁻, they found that [Ga(saltames)]³⁻ and [Al(saltames)]³⁻ were rigid complexes in D₂O solution, whereas [In(saltames)]³⁻ and [Tl(saltames)]³⁻ showed fluxional behavior. The larger metal ions are less easily accommodated by the N₃O₃ tripodal cavity. Because of the imine linkages, the saltames⁶⁻ ligand is much more rigid than TAMS⁶⁻ and presents a tripodal cavity that is more defined within a narrow size range. This can be seen in a comparison of the *pM* values (Table 3). [Ga(saltames)]³⁻ is 7.5 orders of magnitude more stable than [In(saltames)]³⁻. Upon reduction of the imines to amines in TAMS⁶⁻, the difference in the stability between [Ga(TAMS)]³⁻ and [In(TAMS)]³⁻ drops to 4 orders of magnitude. The more flexible TAMS⁶⁻ ligand is better able to accommodate the larger indium(III) ion. [Ga(TAMS)]³⁻ is only 0.5 orders of magnitude more stable than [Ga(saltames)]³⁻, which suggests that the saltames⁶⁻ cavity is well suited to the size of the Ga(III) ion. [Al(saltames)]³⁻ is more stable than [Al(TAMS)]³⁻, which again shows the size preference of the saltames⁶⁻ cavity for the smaller ion and that Al(III) prefers coordination by imine donors over

Table 3. Comparative *pM* Values Calculated at pH = 7.4 (L:M = 10, [M] = 1 μ M)

ligand	Al(III)	Ga(III)	In(III)
TRNS ⁶⁻		22.4	22.1
saltrens ⁶⁻			17.9 $\leq pM \leq$ 21.8 ^a
Sbad ⁴⁻		22.9 ^b	20.1 ^b
TAMS ⁶⁻	15.2	25.1	21.0
saltames ⁶⁻	16.9 ^c	24.6 ^a	17.0 ^a
TAPS ⁶⁻	15.8	24.4	20.4
transferrin	14.5 ^c	20.9 ^d	18.7 ^e
TACN-HP		29.6 ^f	18.4 ^f
TACN-TX		25.9 ^g	15.7 ^g

^a Reference 16. ^b Reference 42. ^c Reference 2. ^d Reference 1. ^e Reference 3. ^f Reference 44. ^g Reference 43.

amine donors. Evans and Jakubovic¹⁶ also gave a *pM* range for [In(saltrens)]³⁻, but their upper limit lies below that of the *pM* for [In(TRNS)]³⁻. Again, this is likely because of the greater flexibility of the amine versus the imine and the fact that TRNS⁶⁻ acts as an N₄O₃ donor toward In(III), whereas saltrens acts as an N₃O₃ donor.

A comparison of the N₃O₃ ligands TAMS⁶⁻ and TAPS⁶⁻ shows similar complexation ability with the three metal ions studied; log *K* for [M(TAMS)]³⁻ and [M(TAPS)]³⁻ are both of the same order of magnitude for a given group 13 metal. The order of stability for both of these ligands with the three group 13 metals is Ga(III) > In(III) > Al(III). This is expected based on literature reports of similar complexes. Martell and co-workers have shown that the oxybenzyl donor displays a large preference for coordinating to gallium(III) over indium(III).⁵ Hancock and co-workers have given estimates for the formation constant of ammonia with the group 13 metals,⁴¹ and these estimates show log *K* trend for M(NH₃)³⁺ formation as In(III) \sim Ga(III) \gg Al(III). On the basis of these reports, one can rationalize the preference of an aminophenolate binding to Ga(III) over In(III) in terms of the presence of the oxybenzyl donor. In the case of Sbad⁴⁻, which is an N₄O₂ donor⁴² (see below), a coordination preference for Ga(III) over In(III) was also observed; however, the *pM* values (Table 3) were decreased by 2 orders of magnitude for Ga(III) and 1 order of magnitude for In(III). The lowering of the stability constants is probably because of the replacement of an anionic oxybenzyl donor by a neutral amino group, and this also leads to a ligand which is less selective for Ga(III) over In(III) relative to TAMS⁶⁻ or TAPS⁶⁻. The same trend (Ga(III) > In(III)) is also observed with TACN-TX⁴³ and TACN-HP⁴⁴ (see below). For these N₃O₃ ligands, the amine backbone is the macrocycle 1,4,7-triazacyclononane, and the selectivity for Ga(III) over In(III) is close to 10 orders of magnitude (Table 3). Comparing the *pM* values of saltames⁶⁻ versus TAMS⁶⁻ shows the dramatic effect of ligand rigidity on the stability of the metal complex, where [In(TAMS)]³⁻ is 10⁴ times more stable than [In(saltames)]³⁻. Presumably, the macrocyclic ring in TACN-HP and TACN-TX is providing a similar effect, *i.e.*, the macrocycle has a clear preference for the smaller Ga(III) ion. This is supported by the fact that although polyaminopolycarboxylates generally favor In(III) complexation over Ga(III) complexation, the aminocarboxylate NOTA shows a large (10⁵) selectivity for Ga(III).⁴⁵

The affinity of the oxybenzyl donor for Al(III) has not been probed in detail; however, the affinity of anionic oxygen donors

(39) Nelson, W. O. Ph.D. Thesis, University of British Columbia, Vancouver, BC, 1988.

(40) Cole, E.; Copley, R. C. B.; Howard, J. A. K.; Parker, D.; Ferguson, G.; Gallagher, J. F.; Kaitner, B.; Harrison, A.; Royle, L. *J. Chem. Soc., Dalton Trans.* **1994**, 1619.

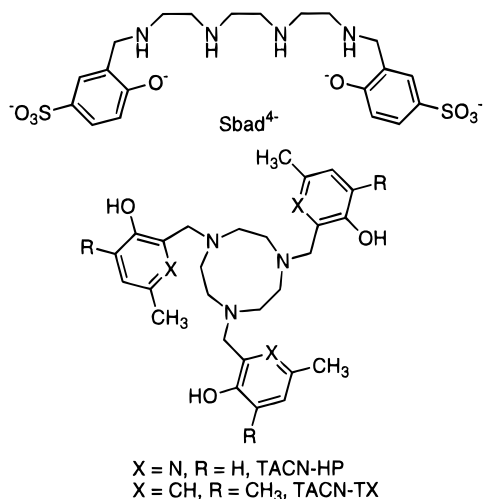
(41) Mulla, F.; Marsicano, F.; Nakani, B. S.; Hancock, R. D. *Inorg. Chem.* **1985**, *24*, 3076.

(42) Wong, E.; Caravan, P.; Liu, S.; Rettig, S. J.; Orvig, C. *Inorg. Chem.* **1996**, *35*, 715.

(43) Clarke, E. T.; Martell, A. E. *Inorg. Chim. Acta* **1991**, *186*, 103.

(44) Motekaitis, R. J.; Sun, Y.; Martell, A. E. *Inorg. Chim. Acta* **1992**, *198–200*, 421.

(45) Clarke, E. T.; Martell, A. E. *Inorg. Chim. Acta* **1991**, *181*, 273.



for Al(III) is axiomatic. The low stabilities of the Al(III) complexes studied here, relative to their Ga(III) and In(III) analogs, are likely because of the low affinity of Al(III) for the neutral amine donor. A consequence of this weak amine affinity is that the protonated complexes, [Al(HTAPS)]²⁻ and [Al(HTAMS)]²⁻, exist over a broader pH range than do their Ga(III) or In(III) analogs. By analogy with [Ga(HTAPS)]²⁻, one of the amine groups remains protonated and Al(III) is coordinated by an N₂O₃ donor set with the last octahedral coordination site occupied by a water molecule.

The preference of Al(III) for anionic oxygen donors coupled with the fact that TAMS⁶⁻ and TAPS⁶⁻ failed to prevent some Al(III) hydrolysis makes it hardly surprising that no stability constants in the Al-TRNS system were obtained. The crystal structure of the nonsulfonated analog¹⁸ (Scheme 2) had one of the secondary amines protonated and uncoordinated. A result of this N₃O₃ donor set is that the stable six-membered chelate ring formed with 2-oxybenzylamino coordination is lost for one of the three arms. This lack of chelate ring stability coupled with the larger size of the TRNS backbone make this ligand useless for Al(III) coordination. The factors which disfavor Al(III) complexation by TRNS⁶⁻ serve to make TRNS⁶⁻ the best ligand in this series for the coordination of In(III). Indium is large enough to accommodate all seven donor atoms, resulting in the formation of three six-membered and three five-membered chelate rings. The optimization of all seven donors coupled with the larger cavity size of TRNS⁶⁻ and the higher affinity of In(III) for amine donors results in a ligand that coordinates In(III) as well as it does Ga(III). The coordination of Ga(III) by TRNS⁶⁻ gives an N₄O₂ coordination geometry, and this results in a *pM* value lower than that in the N₃O₃ donors studied here, but of the same order of magnitude as that in Sbad⁴⁻, another N₂O₄ aminophenolate donor.⁴² The Ga(III) ion is too small to be seven coordinate. By binding in an N₄O₂ fashion, the complex optimizes the number of five- and six-membered chelate rings formed (three five-membered and two six-membered rings). Although an N₃O₃ donor set would be better suited to Ga(III), TRNS⁶⁻ can only accomplish this by breaking up part of its chelate ring network.

This may represent a useful result in the selectivity of In(III) over Ga(III). Recently Martell, Welch, and co-workers have focused on developing chelators with a high affinity for In(III) and have had some success by incorporating thiol donors.⁴⁶⁻⁵⁰

Ligand design incorporating seven or eight donors would enhance In(III) selectivity by yielding an In(III) complex with a coordination number greater than six and lead to steric congestion by the noncoordinating donors in the analogous Ga(III) complex. This has also been shown recently in stability constant studies involving dtpa derivatives.⁵¹

All of the ligands reported here, with the exception of TACS⁶⁻, form more stable complexes with Ga(III) and In(III) at pH = 7.4 than does transferrin. From a thermodynamic standpoint, the aminophenolates based on tame and tap represent the best candidates for a ligand framework with which to design ⁶⁷Ga radiopharmaceuticals. The tren backbone is better suited for In(III), but the use of oxybenzyl donors should be avoided for ¹¹¹In radiopharmaceuticals, and these should be replaced with thiolates.

H₆TACS proved to be the poorest candidate of this series for group 13 metal sequestration. The only metal examined was Ga(III); on the basis of the results obtained with the Ga-TAMS and Ga-TAPS titrations, it is expected that Ga(III) might form a stable group 13 metal complex with TACS⁶⁻. The complexation kinetics were very slow, however, and the ligand was incapable of preventing some precipitation of Ga(OH)₃ upon standing for 3 months. Using the solubility product of amorphous Ga(OH)₃³² and the deprotonation constants for H₆TACS, an upper limit for [Ga(TACS)]³⁻ formation can be determined to be log *K* = 30. From a thermodynamic viewpoint only, this means that complexation might not start until above pH = 4 and that Ga(OH)₄⁻ would start to form at pH = 10. This is a result of the higher basicity of TACS⁶⁻ relative to that of TAMS⁶⁻. Furthermore, complexation must take place with the energetically disfavored axial conformer. If the free ligand existed in the axial conformer, there would be a gain in the energy of complex formation in the amount of the energy difference between the two conformers. This has been shown for M(II) complexes of tame and tach.^{36,52} Both of these tris-(amine) ligands bind in a facial manner, and both have stability constants of the same order of magnitude for Ni(II), Cu(II), and Zn(II).^{36,52} Paoletti and co-workers showed that the similarity in binding constants is because of a coincidence between an unfavorable enthalpy change and a favorable entropy change when tach coordinates to a metal.⁵³ The amine tach, when in the axial conformation, is preorganized for binding, and this results in a more positive entropy relative to tame. In order to achieve this conformation, tach must undergo a ring-flip to a conformer higher in energy; it is this unfavorable enthalpy process which nullifies the gain in entropy. Parker and co-workers have recently prepared the conformationally biased *cis,cis*-2,4,6-trimethyl-1,3,5-triaminocyclohexane ligand in which the three amino groups are in the axial conformation.⁵⁴ They have also prepared the tris(2-hydroxybenzyl) derivative as well as the aminocarboxylate and aminophosphinate derivatives.⁵⁴

(47) Li, Y.; Martell, A. E.; Hancock, R. D.; Riebenspies, J. H.; Anderson, C. J.; Welch, M. J. *Inorg. Chem.* **1996**, *35*, 404.

(48) Ma, R.; Welch, M. J.; Riebenspies, J.; Martell, A. E. *Inorg. Chim. Acta* **1995**, *236*, 75.

(49) Sun, Y.; Motekaitis, R. J.; Martell, A. E.; Welch, M. J. *Inorg. Chim. Acta* **1995**, *228*, 77.

(50) Sun, Y.; Anderson, C. J.; Pajeau, T. S.; Reichert, D. E.; Hancock, R. D.; Motekaitis, R. J.; Martell, A. E.; Welch, M. J. *J. Med. Chem.* **1996**, *39*, 458.

(51) Hancock, R. D.; Cukrowski, I.; Cukrowska, E.; Hosken, G. D.; Iccharam, V.; Brechbiel, M. W.; Gansow, O. A. *J. Chem. Soc., Dalton Trans.* **1994**, 2679.

(52) Sabatini, A.; Vacca, A. *J. Chem. Soc., Dalton Trans.* **1980**, 519.

(53) Fabbrizzi, L.; Micheloni, M.; Paoletti, P. *J. Chem. Soc., Dalton Trans.* **1980**, 1055.

(54) de Angelis, S.; Batsanov, A.; Norman, T. J.; Parker, D.; Senanyake, K.; Vepsäläinen, J. *J. Chem. Soc., Chem. Commun.* **1995**, 2361.

(46) Anderson, C. J.; John, C. S.; Li, Y. J.; Hancock, R. D.; McCarthy, T. J.; Martell, A. E.; Welch, M. J. *Nucl. Med. Biol.* **1995**, *22*, 165.

An aminophenolate ligand based on this amine should exhibit high-formation constants with trivalent metal ions because of the favorable entropy that is associated with its preorganization, while the unfavorable enthalpic effect in tach derivatives is eliminated because no conformational change is necessary for binding. The lack of a conformational change on binding should also serve to increase the kinetics of complexation.

Conclusions

The tripodal framework offers intermediate chelation properties between open chain ligands and those based on macrocycles. ^1H NMR gives some evidence for preorganization in the TAPS system, and this is likely present in the TRNS and TAMS systems as well. The order of the stabilities for a given ligand are $\text{Ga} > \text{In} > \text{Al}$. The low affinity of Al(III) for amine donors coupled with slow complexation kinetics makes these ligands unsuitable for Al(III) sequestration. The presence of the oxybenzyl donor imparts a selectivity for Ga(III) over In(III); TAMS $^{6-}$ and TAPS $^{6-}$ are best suited for Ga(III) complexation. The larger ligand cavity and the seven donor atoms of TRNS $^{6-}$

make it the best ligand for In(III). The solid state structures determined for the Ga(III) and In(III) complexes of the nonsulfonated analogs of TRNS,¹⁸ TAMS,²¹ and TAPS²⁰ are retained in aqueous solution. This parallel is absent for Al(III); Al(III) has a greater propensity for forming protonated complexes with TAMS and TAPS, and no stable complex was observed with TRNS, reinforcing the importance of water and/or hydroxide as a ligand in aqueous Al(III) chemistry. TACS exists in the wrong conformation for metal ion complexation, and as a result, TACS exhibits exceedingly slow complexation kinetics and weaker binding.

Acknowledgment. This work was supported by the BC Health Research Foundation and the Natural Sciences and Engineering Research Council (NSERC) of Canada. P.C. acknowledges NSERC of Canada for a postgraduate scholarship (1992–1996), and the authors thank Professor L. S. Weiler and Dr. M. Ivery for the results of the MM3 calculations on tach.

IC961222U